

# รายงานวิจัยฉบับสมบูรณ์

โครงการ การผลิตและทำให้ไฮโครเจนบริสุทธิ์จากเอธานอลที่ได้จากชีวภาพ โดยใช้การแปรรูป ด้วยไอน้ำ สำหรับใช้ในเซลเชื้อเพลิง

โดย อมรมาศ ศิริจารุพันธุ์ และคณะ

# รายงานวิจัยฉบับสมบูรณ์

โครงการ การผลิตและทำให้ไฮโครเจนบริสุทธิ์จากเอธานอลที่ได้จากชีวภาพ โดยใช้การแปรรูป ด้วยไอน้ำ สำหรับใช้ในเซลเชื้อเพลิง

คณะผู้วิจัย สังกัด

1. อมรมาศ ศิริจารุพันธุ์ มหาวิทยาลัยเทคโนโลยีพระจอมเกล้าธนบุรี

2. ปียะสาร ประเสริฐธรรม จุฬาลงกรณ์มหาวิทยาลัย

สนับสนุนโดยสำนักงานคณะกรรมการอุดมศึกษา และสำนักงานกองทุนสนับสนุนการวิจัย (ความคิดเห็นในรายงานนี้เป็นของผู้วิจัย สกอ. และ สกว. ไม่จำเป็นต้องเห็นด้วยเสมอไป)

#### บทคัดย่อ

้ เชื้อเพลิงที่ได้จากชีวมวล เป็นอีกทางเลือกหนึ่งของแหล่งพลังงานที่เป็นมิตรกับสิ่งแวดล้อม เอธานอลสามารถผลิตได้จากกระบวนการหมักของชีวมวล และสามารถถกปฏิรปด้วยไอน้ำเป็น ใชโดรเจน เมื่อมีตัวเร่งปฏิกิริยาที่เหมาะสม เพื่อใช้ในเซลเชื้อเพลิง ในช่วงแรกของการศึกษา ตัวเร่ง ปฏิกิริยาโคบอลต์บนตัวรองรับซิลิกา โคยมีปริมาณโคบอลต์ 10 เปอร์เซ็นต์โคยน้ำหนัก ถูกศึกษาเพื่อหา ความเข้มข้นที่เหมาะสมของเอธานอล ในการทำปฏิกิริยาปฏิรูปด้วยไอน้ำ โดยเปลี่ยนความเข้มข้นของ เอธานอลจาก 15% เป็น 20% และ 25% โดยปริมาตร ที่อณหภมิ 450°C และความคันบรรยากาศ ผลการ ทคลองแสคงให้เห็นว่า ถึงแม้ว่าไฮโครเจนที่ผลิตได้มีปริมาณเพิ่มขึ้นเมื่อเพิ่มความเข้มข้นของเอธานอล ในรูปของผลผลิต (yield) กลับมีค่าลดลง ซึ่งสื่อเป็นนัยว่าสัดส่วนของเอธานอลที่ถูกเปลี่ยนเป็น ใชโครเจนมีค่าลดลง เมื่อเพิ่มความเข้มข้นของเอธานอล และแสคงให้เห็นในรูปของค่าการเลือกของ ไฮโครเจนที่ลคลง ในทางตรงข้าม ค่าการเลือกของคาร์บอนมอนนอกไซค์ มีค่าค่อนข้างคงที่กับความ เข้มข้นของเอธานอล ดังนั้นในเชิงคุณภาพของผลิตภัณฑ์ และผลผลิตของไฮโครเจน ความเข้มข้นของ เอธานอลที่ 15% โดยปริมาตรดูเหมือนเป็นสภาวะที่ดีที่สุดในการปฏิรูปด้วยใอน้ำของเอธานอล ผลการ ทคลองนี้สื่อเป็นนัยว่า เอธานอลที่ได้จากการหมักชีวมวลสามารถนำไปใช้ได้โดยตรง โดยไม่ต้องผ่าน กระบวนการกลั่น นอกจากนั้น เนื่องจากตัวเร่งปฏิกิริยามีราคาค่อนข้างแพง การพิจารณาดีกรีการใช้ ประโยชน์ของตัวเร่งปฏิกิริยาจึงเป็นอีกสิ่งหนึ่งที่น่าสนใจ ค่าความถี่ในการหมุนเวียนที่มีค่าสูง ที่ความ เข้มข้นของเอธานอลสูง หมายความว่าตัวเร่งปฏิกิริยาถูกใช้ประโยชน์มากขึ้นเมื่อความเข้มข้นของ เอธานอลสูงขึ้น เมื่อเพิ่มปริมาณ โคบอลต์เป็น 20% โดยน้ำหนัก ผลการทคลองพบว่าคุณภาพของ ผลิตภัณฑ์ดีขึ้น นอกจากนั้น ความถี่ในการหมุนเวียนของตัวเร่งปฏิกิริยา 10% และ 20% Co/SiO, ที่ สภาวะเดียวกัน มีค่าเท่าๆ กัน ดังนั้นปฏิกิริยาการปฏิรูปด้วยไอน้ำของเอธานอลจึงเป็นปฏิกิริยาที่ไม่ไว ต่อโครงสร้างของตัวเร่งปฏิกิริยา เนื่องจากไม่ขึ้นกับขนาคอนุภาคของตัวเร่งปฏิกิริยา และที่อุณหภูมิ เดียวกัน ความว่องไวของจุดกัมมันต์ของโคบอลต์เปลี่ยนแปลงกับความเข้มข้นของเอธานอลเท่านั้น ไม่ เปลี่ยนกับปริมาณ โคบอลต์ในตัวเร่งปฏิกิริยา ผลการทดลองในการศึกษาการเสื่อมสภาพของตัวเร่ง ปฏิกิริยา หลังจากใช้ในปฏิกิริยาเป็นเวลา 6 ชั่วโมง ไม่พบการรวมตัวของตัวรองรับซิลิกาจากความร้อน แต่พบการลคลงเล็กน้อยของปริมาตรรูพรุน และขนาครูพรุนซึ่งเป็นไปได้ว่าเกิดขึ้นเพราะการก่อตัวของ โค้กภายในรูพรุนขนาดกลาง

สัดส่วนองค์ประกอบของผลิตภัณฑ์ในก๊าซแห้งที่สภาวะสมคุลทางเทอร์โมไดนามิกส์ เมื่อ เปลี่ยนอุณหภูมิของปฏิกิริยา และอัตราส่วนใอน้ำต่อเอธานอล ถูกคำนวณโดยใช้วิธี Lagrange's undetermined multipliers เพื่อหาสัดส่วนองค์ประกอบที่ทำให้ผลรวมพลังงานกิปส์ของระบบมีค่าต่ำ ที่สุด จากนั้นนำผลที่ได้มาเปรียบเทียบกับผลที่ได้จากวิธีที่ถูกเสนอโดย Mas et al. [1] โดยการสมมุติชุด ของปฏิกิริยาที่เป็นอิสระต่อกันขึ้นมาชุดละ 3 ปฏิกิริยา สำหรับ 2 รูปแบบปฏิกิริยา เพื่อให้สามารถ

อธิบายผลการทดลองได้ดียิ่งขึ้น อีกหนึ่งรูปแบบปฏิกิริยาได้ถูกเสนอขึ้นมาในการศึกษานี้ ทั้งสาม รูปแบบปฏิกิริยาประกอบด้วย 1) ปฏิกิริยาการเปลี่ยนเอธานอล 2) ปฏิกิริยา water-gas-shift และ 3) ปฏิกิริยาการปฏิรูปมีเทนด้วยไอน้ำ ความแตกต่างของแต่ละรูปแบบปฏิกิริยาคือ เส้นทางการเปลี่ยน เอธานอล โดยเกิดจากการสลายตัวของเอธานอล ในรูปแบบ A, ถูกปฏิรูปด้วยไอน้ำเกิดเป็นมีเทน คาร์บอนไดออกไซด์ และ 2 โมลของไฮโดรเจน ในรูปแบบ B, และ ถูกปฏิรูปด้วยไอน้ำแกิดเป็น 2 โม ลของ คาร์บอนมอนนอกไซค์ และ 3 โมลของไฮโครเจน ในรูปแบบ  $\mathbf C$  ไม่น่าประหลาดใจเลยว่า สัดส่วนองค์ประกอบที่สมคุลที่กำนวณได้จากวิธีทั้งสอง มีค่าเท่ากันที่สภาวะเดียวกัน ปริมาณไฮโดรเจน และคาร์บอนมอนนอกไซด์ในผลิตภัณฑ์ เพิ่มขึ้นกับอุณหภูมิของปฏิกิริยา ในทางตรงกันข้าม ปริมาณ คาร์บอนใดออกไซด์และมีเทน มีค่าลดลงเมื่อเพิ่มอุณหภูมิ ในขณะที่ปริมาณไฮโดรเจนเพิ่มขึ้นเมื่อ ้อัตราส่วนของไอน้ำต่อเอธานอลเพิ่มขึ้น ปริมาณการ์บอนมอนนอกไซด์กลับมีค่าลดลง ผลการทดลองนี้ แนะนำว่า เพื่อผลิต ใฮโครเจนให้ ได้มากที่สุดและคาร์บอนมอนนอกไซค์น้อยที่สุด ต้องทำการปรับ อัตราส่วนของไอน้ำต่อเอธานอลให้เหมาะสม ในการคำเนินการจริง สัคส่วนองค์ประกอบของ ผลิตภัณฑ์จะขึ้นกับความว่องไวของตัวเร่งปฏิกิริยา ตัวอย่างเช่น ถ้าตัวเร่งปฏิกิริยาไม่ว่องไวต่อปฏิกิริยา water-gas-shift เลย คาร์บอนไดออกไซด์จะไม่สามารถเกิดขึ้นได้ และจากการคำนวณ ปริมาณคาร์บอน มอนนอกไซด์จะมีค่าคงที่ที่สมดุล ไม่ว่าอุณหภูมิหรืออัตราส่วนของไอน้ำกับเอธานอลจะเปลี่ยนไป อย่างไร ที่อุณหภูมิสูงพอในการผลิตไฮโดรเจน ก๊าซที่ออกจากเตาปฏิรูปต้องถูกบำบัดในเตาปฏิกรณ์ Low-temperature shift ก่อนนำไปใช้ในเซลเชื้อเพลิง สัดส่วนองค์ประกอบที่สมคุลของก๊าซที่ออกจาก เตาปฏิกรณ์ Low-temperature shift ที่อุณหภูมิ 473 K ถูกคำนวณ โดยใช้สมมุติฐานว่าตัวเร่งปฏิกิริยานั้น ว่องไวเฉพาะกับปฏิกิริยา water-gas-shift เท่านั้น ผลการคำนวณแสดงให้เห็นว่า สำหรับกระแสของ ใฮโครเจนที่มีปริมาณคาร์บอนมอนนอกไซค์ที่ยอมรับได้ เพื่อใช้ในเซลเชื้อเพลิงแบบ solid oxide ถ้า อัตราส่วนของไอน้ำต่อเอธานอลมากกว่าหรือเท่ากับ 9 อุณหภูมิในเตาปฏิรูปจะเป็นเท่าไรก็ได้ แต่ถ้า อัตราส่วนของไอน้ำต่อเอธานอลต่ำกว่านั้น อุณหภูมิจะต้องต่ำลง เช่น เมื่ออัตราส่วนของไอน้ำต่อ เอธานอลเท่ากับ 3 อุณหภูมิต้องต่ำกว่า 950 K ในการใช้กับเซลเชื้อเพลิงแบบ PEM ช่วงในการ คำเนินการของเตาปฏิรูปจะแกบลง โดยมีแก่ช่วงเดียวคือ อุณหภูมิต่ำกว่า 623 K และ อัตราส่วนของไอ น้ำต่อเอธานอล มากกว่าหรือเท่ากับ 18 แต่ผลผลิตของไฮโครเจนมีค่าน้อยมากที่สภาวะนี้ คังนั้นการใช้ เฉพาะการปฏิรูปด้วยใอน้ำและปฏิกิริยา Low-temperature shift จึงไม่เพียงพอในการผลิตไฮโดรเจนเพื่อ ใช้ในเซลเชื้อเพลิงแบบ PEM ปริมาณคาร์บอนมอนนอกไซค์สามารถลดลงให้อย่ในระดับไม่กี่ส่วนใน ล้านส่วนได้ โดยใช้เตาปฏิกรณ์การเลือกออกซิไดซ์คาร์บอนมอนนอกไซด์ ซึ่งจากการศึกษาที่ผ่านมา พบว่าตัวเร่งปฏิกิริยาแพลทินัม และทอง มีความเหมาะสมสำหรับวัตถุประสงค์นี้ น้ำหนักของตัวเร่ง ปฏิกิริยาเพื่อลดปริมาณการ์บอนมอนนอกไซด์ลงให้อยู่ในระดับไม่กี่ส่วนในล้านส่วน ถูกคำนวณโดยใช้ ข้อมูลความว่องไวและค่าการเลือกจากการศึกษาที่ผ่านมา และพบว่ามีค่าเพิ่มขึ้นเมื่ออุณหภูมิในเตา ปฏิรูปเพิ่มขึ้น หรืออัตราส่วนระหว่างไอน้ำกับเอธานอลลคลง คังนั้น ในการออกแบบกระบวนการผลิต ไฮโดรเจนโดยการปฏิรูปเอธานอลด้วยไอน้ำ ต้องคำนึงถึงขนาดของเตาปฏิรูปซึ่งเพิ่มขึ้นเมื่อเพิ่ม อัตราส่วนระหว่างไอน้ำกับเอธานอล และขนาดของเตาปฏิกรณ์การเลือกออกซิไดซ์คาร์บอนมอนนอก ไซด์รวมถึงค่าใช้จ่ายในการซื้อตัวเร่งปฏิกิริยา ซึ่งเป็นไปในทางตรงข้าม คือลดลงเมื่อเพิ่มอัตราส่วน ระหว่างไอน้ำกับเอธานอล

หลังจากการกำนวณสัดส่วนองก์ประกอบของผลิตภัณฑ์ในก๊าซแห้งที่สภาวะสมคุลทางเทอร์โม ใดนามิกส์แล้ว ได้ทำการศึกษาการเข้าสู่สมคุลเมื่อใช้ตัวเร่งปฏิกิริยาโคบอลต์ โรเดียม และ นิกเกิล ข้อมูลจากการทดลองที่ได้จากแหล่งต่างๆ ถูกนำมาใช้ในการเปรียบเทียบ ข้อมูลบางส่วนถูกคำนวณใหม่ ในอยู่ในรูปของสัดส่วนองค์ประกอบของผลิตภัณฑ์ในก๊าซแห้ง และจำนวณโมลของไฮโดรเจนต่อโม ลของเอธานอลที่ถูกเปลี่ยน การเปรียบเทียบแสดงให้เห็นว่าเส้นทางการเปลี่ยนเอธานอลสำหรับตัวเร่ง ปฏิกิริยาโคบอลต์และนิกเกิลที่อุณหภูมิต่ำกว่า 873 K เกิดโดยการปฏิรูปเพิ่มขึ้น เส้นทางการเปลี่ยนเอธานอล เปลี่ยนเป็นรูปแบบ A การสลายตัวของเอธานอลสำหรับตัวเร่งปฏิกิริยาโคบอลต์ และรูปแบบ B ปฏิรูป ด้วยไอน้ำเป็นมีเทน คาร์บอนไดออกไซด์ และไฮโดรเจน สำหรับตัวเร่งปฏิกิริยานิกเกิล การ เปลี่ยนแปลงนี้ อาจเนื่องมาจากการลดลงของความว่องไวในการเร่งปฏิกิริยาการปฏิรูปมีเทนด้วยไอน้ำ สำหรับตัวเร่งปฏิกิริยาทั้งสอง เมื่ออุณหภูมิสูงขึ้น ถ้าตัวเร่งปฏิกิริยามีความว่องไวเพียงพอต่อปฏิกิริยา water-gas-shift เส้นทางการเปลี่ยนเอธานอลจะเปลี่ยนเป็นรูปแบบ B แต่ถ้าไม่ จะกลายเป็นรูปแบบ A เป็นที่น่าเสียดายที่ไม่มีข้อมูลเกี่ยวกับตัวเร่งปฏิกิริยาโรเดียมที่อุณหภูมิต่ำ ดังนั้นจึงสามารถสรุปได้เพียงว่า บนตัวเร่งปฏิกิริยาโรเดียมที่อุณหภูมิสูงกว่า 923 K เอธานอลถูกเปลี่ยนโดยรูปแบบ B และไม่ขึ้นกับ อัตราร่างไรนี้กับเอธานอล

#### **Abstract**

Fuel derived from biomass is an environmental friendly alternative of energy source. The ethanol can be obtained from the fermentation process, and can be steam reformed to hydrogen in the presence of suitable catalyst, to be further used in fuel cells. In the first part of this study, the Co/SiO<sub>2</sub> catalyst with 10% cobalt loading was preliminary studied to determine the suitable concentration of ethanol during the steam reforming. The ethanol concentration was varied from 15%, to 20% and 25% by volume at 450°C reaction temperature and atmospheric pressure. The results showed that although the amount of hydrogen generated increased with ethanol concentration, in term of hydrogen yield it decreased. It implied that smaller fraction of ethanol was converted to hydrogen at higher ethanol concentration, as shown by the decreased in hydrogen selectivity. On the other hand, the selectivity toward carbon monoxide was nearly constant with ethanol concentration. Thus, in term of product gas quality and hydrogen yield, 15% ethanol by volume seems to be the best condition for ethanol steam reforming. This result implied that bio-ethanol from fermentation process can be directly used without distillation step. Since this catalyst is quite expensive, it would be interesting to consider the degree of utilization of the catalyst. The turnover frequency showed that higher turnover frequency was obtained at higher ethanol concentration meaning that catalyst was more utilized at higher concentration of ethanol. When increasing the cobalt loading to 20%, it was found that the product quality was improved. In addition, the turnover frequency of the 10% and 20% Co/SiO<sub>2</sub> were approximately the same at the same reaction condition, thus, the steam reforming of ethanol is the structural insensitive reaction. It suggested that at the same reaction temperature, site activity of cobalt metals varies only with the concentration of ethanol, not the percent loading. Results from the deactivation study after 6 hours of reaction showed no sintering of silica support but a slight decrease in pore volume and pore size was observed, probably by a slight coke formation inside the mesopores.

The composition of dry gas product at equilibrium when varying reaction temperature and steam/ethanol ratio was calculated using Lagrange's undetermined multipliers. The results were later compared with the one obtained from the method proposed by Mas et al. [1] by assuming a set of three independent reactions for each reaction scheme. To better explain the experimental results, one more scheme was proposed in this study. All three schemes were composed of i) ethanol conversion reaction, ii) water-gas-shift reaction and iii) methane steam reforming reaction. The difference of each scheme is the ethanol conversion path, which is via ethanol decomposition in scheme A, via steam reforming to methane, carbon dioxide and 2 moles

of hydrogen in scheme B, and via steam reforming to 2 moles of carbon monoxide and 4 moles of hydrogen in scheme C. Unsurprisingly, the equilibrium composition obtained from two methods was the same at the same condition. The amount of hydrogen and carbon monoxide in dry gas product increased with reaction temperature. While the amount of hydrogen increased with steam/ethanol ratio, that of carbon monoxide decreased. In contrast, the amount of carbon dioxide and methane decreased with reaction temperature. This result suggested that although high temperature has positive effect on the amount of hydrogen generated, it also increases the amount of carbon monoxide, the undesired product. Therefore, in order to maximize the production of hydrogen and minimize the amount of carbon monoxide, the steam/ethanol ratio must be adjusted. In actual operation, the composition of dry gas product would depend on the activity of the reformer catalyst. For example, if the catalyst is not active at all for water-gas-shift reaction, carbon dioxide cannot be generated and the amount of carbon monoxide will be constant with reformer temperature and steam/ethanol ratio. At temperature high enough for hydrogen production, the reformer effluent gas must be treated in Low-temperature shift reactor before being used in fuel cell. Catalysts used in shift reactor are normally active only for this reaction. The equilibrium composition of the effluent gas after the Low-temperature shift reaction at 473 K was calculated. The results showed that for hydrogen stream with tolerable amount of carbon monoxide to be used in solid oxide fuel cell, any reformer temperature can be used if steam/ethanol ratio is higher than 9. At low steam/ethanol ratio such as 3, reformer temperature has to be lower than ~950 K. The reformer conditions are much narrower to be used in PEM fuel cell. The only possible condition is reformer temperature below 623 K and steam/ethanol ratio equal or higher than 18 but low hydrogen yield will be obtained at this condition. Therefore, only steam reformer and low-temperature shift reactor are not enough to produce hydrogen stream suitable to be used with PEM fuel cell. With the help from selective oxidation reactor, the amount of carbon monoxide can be reduced to only a few ppm. Many studies showed that Pt and Au- based catalysts are suitable catalysts for this purpose. The catalyst weights when using Pt-based and Au-based catalyst were calculated. They were found to depend on the catalytic activity and selectivity and increased with an increase in reformer temperature and a decrease in steam/ethanol ratio. Therefore, during the process design for hydrogen production using ethanol steam reforming, size of reformer, which is larger at higher steam/ethanol ratio, and the size of the selective oxidation reactor, larger at low steam/ethanol ratio, must be traded off.

After the equilibrium composition of dry gas reformer product was calculated, the approach to equilibrium when using cobalt, rhodium, and nickel-based catalysts was investigated. The experimental data obtained from various sources were used in the comparison. Some of these data were recalculated to the percentage of main components

in dry gas product and the number of moles of hydrogen generated per mole of converted ethanol. The comparison showed that the possible ethanol conversion path for Co and Ni-based catalyst seemed to be via scheme C, steam reforming to CO and H<sub>2</sub>, at low temperature. When the reformer temperature was increased, the ethanol conversion path changed to scheme A, ethanol decomposition, for Co-based catalysts and to scheme B, steam reforming to CH<sub>4</sub>, CO<sub>2</sub> and H<sub>2</sub> for Ni-based catalysts. This might be because of the decreasing activity toward methane steam reforming for both catalysts at higher temperature. In scheme C, the methane steam reforming occurs simultaneously with the ethanol decomposition reaction of Co. When the methane steam reforming activity decreased, if that catalyst has sufficient activity toward water-gas shift reaction, the ethanol conversion path will change to scheme B, if not, it will change to scheme A. Unfortunately, data at low temperature are not available for Rh-based catalysts. The only conclusion for these catalysts is that at high temperature, ethanol was converted via scheme B and it is independent of the steam/ethanol ratio.

# **Executive Summary**

Main fuels used at present come from crude oil refinery. This energy source is limited and will be extinguish within a few decades. This necessity forces researchers to look for other alternative fuels. Fuel derived from biomass is an environmental friendly alternative of energy source. The fermentation process can be incorporated to produce ethanol, which can be steam reformed to hydrogen in the presence of suitable catalyst and then further used in fuel cells. In the first part of this study, the Co/SiO<sub>2</sub> catalyst with 10% cobalt loading was preliminary studied to determine the suitable concentration of ethanol during the steam reforming. The ethanol concentration was varied from 15%, to 20% and 25% by volume at 450°C reaction temperature and atmospheric pressure. In addition the effect of metal loading was also studied by increasing %metal loading to 20%. Both 10% and 20% Co/SiO<sub>2</sub> were prepared by the incipient wetness impreganation method using Co(NO<sub>3</sub>)<sub>2</sub> as the cobalt precursor. The catalysts were dried at 110°C for 6 h and calcined in static air at 350°C for 2 h. The BET surface area, pore volume and pore size of the calcined catalysts were measured by a Quantachrome Autosorb-1 instrument. To determine the phase of the calcined catalysts, the powder X-ray diffraction in the JOEL X-Ray diffractometer was used. The metal dispersion and corresponding metal particle size of catalyst after reduction was measured and calculated using pulse chemisorption instrument. The characterization showed the decrease in BET surface area, pore volume, pore size and %metal dispersion with %metal loading, corresponding to the increase in metal particle size. This implied the occurrence of the blockage of some silica mesopores by cobalt particles. The X-Ray diffraction showed that the main phase in calcined Co/SiO<sub>2</sub> catalyst was Co<sub>3</sub>O<sub>4</sub>, as expected. Results from the ethanol steam reforming experiment showed that the main products in dry gas consisted of hydrogen, carbon dioxide, carbon monoxide and methane. Their production amounts all increased when increasing ethanol concentration. Although the amount of hydrogen generated increased with ethanol concentration, in term of hydrogen yield it decreased. It implied that smaller fraction of ethanol was converted to hydrogen at higher ethanol concentration, as shown by the decreased in hydrogen selectivity. On the other hand, the selectivity toward carbon monoxide was nearly constant with ethanol concentration. Thus, in term of product gas quality and hydrogen yield, 15% ethanol by volume seems to be the best condition for ethanol steam reforming. This result implied that bio-ethanol from fermentation process can be directly used without distillation step. However, size of reformer must be larger when using more dilute ethanol and larger heat supply is required. Since this catalyst is quite expensive, it would be interesting to consider the degree of utilization of the catalyst. The turnover frequency showed that higher turnover frequency was obtained at higher ethanol concentration meaning that catalyst was more utilized at higher

concentration of ethanol. When increasing the cobalt loading to 20%, it was found that the product quality was improved. In addition, the turnover frequency of the 10% and 20% Co/SiO<sub>2</sub> were approximately the same at the same reaction condition, thus, the steam reforming of ethanol is the structural insensitive reaction. It suggested that at the same reaction temperature, site activity of cobalt metals varies only with the concentration of ethanol, not the percent loading. Results from the deactivation study after 6 hours of reaction showed no sintering of silica support but a slight decrease in pore volume and pore size was observed, probably by a slight coke formation inside the mesopores.

The composition of dry gas product at equilibrium when varying reaction temperature and steam/ethanol ratio was calculated using the method of Lagrange's undetermined multipliers to minimize the total Gibbs energy of the system. The results were later compared with the one obtained from the method proposed by Mas et al. [1] by assuming two reaction schemes each with a set of three independent reactions. To better explain the experimental results, one more scheme was proposed in this study. These three schemes were composed of the ethanol conversion reaction followed by two competitive reactions; water-gas-shift reaction and methane steam reforming reaction. The difference among these schemes is the ethanol conversion path, which is via ethanol decomposition in scheme A, via steam reforming to methane, carbon dioxide and 2 moles of hydrogen in scheme B, and via steam reforming to 2 moles of carbon monoxide and 4 moles of hydrogen in scheme C. The difference in ethanol conversion path resulted in the difference in the initial moles of each species in the reaction gas during the calculation. Unsurprisingly, the equilibrium composition obtained from these two methods was the same at the same condition. The amount of hydrogen and carbon monoxide in dry gas product increased with reaction temperature. While the amount of hydrogen increased with steam/ethanol ratio, that of carbon monoxide decreased. In contrast, the amount of carbon dioxide and methane decreased with reaction temperature. This result suggested that although high temperature has positive effect on the amount of hydrogen generated, it also increases the amount of carbon monoxide, the undesired product. Therefore, in order to maximize the production of hydrogen and minimize the amount of carbon monoxide, the steam/ethanol ratio must be sufficient. In actual operation, the composition of dry gas product would depend on the activity of the reformer catalyst. For example, if the catalyst is not active at all for water-gas-shift reaction, carbon dioxide cannot be generated and from the equilibrium calculation, the amount of carbon monoxide will be constant, independent of reformer temperature and steam/ethanol ratio. At temperature high enough for hydrogen production, the reformer effluent gas must be treated in Low-temperature shift (LTS) reactor before being used in fuel cell. Catalysts used in LTS reactor are normally active only for this reaction. The equilibrium composition of the effluent gas

after the LTS shift reaction at 473 K was calculated based on this fact. The results showed that to produce hydrogen stream with tolerable amount of carbon monoxide to be used in solid oxide fuel cell, any reformer temperature can be used if steam/ethanol ratio is equal to or higher than 9. At low steam/ethanol ratio such as 3, reformer temperature has to be lower than ~950 K. The reformer conditions are much narrower for hydrogen to be used in PEM fuel cell. The only possible condition is reformer temperature below 623 K and steam/ethanol ratio equal to or higher than 18 but low hydrogen yield will be obtained at this condition. Therefore, only steam reformer and low-temperature shift reactor are not enough to produce hydrogen stream suitable to be used with PEM fuel cell. With the help from selective oxidation reactor, the amount of carbon monoxide can be reduced to only a few ppm. Many studies showed that Pt and Au- based catalysts are suitable catalyst for this purpose. The catalyst weights when using Pt-based and Au-based catalyst were calculated from available reported data. They were found to depend on the catalytic activity and selectivity and increase with an increase in reformer temperature and a decrease in steam/ethanol ratio. The smallest catalyst weight was found when using Au/y-Al<sub>2</sub>O<sub>3</sub> catalyst, which had high activity and selectivity toward CO oxidation. Therefore, during the process design for hydrogen production using ethanol steam reforming, size of reformer, which is larger at higher steam/ethanol ratio, and the size of the selective oxidation reactor, larger at low steam/ethanol ratio, must be traded off.

After the equilibrium composition of dry gas reformer product was calculated, the approach to equilibrium when using cobalt, rhodium, and nickel-based catalysts was investigated. The experimental data obtained from various sources were used in the comparison. Some of these data were recalculated to the percentage of main components in dry gas product and the number of moles of hydrogen generated per mole of converted The comparison showed that the possible ethanol conversion path for Co and Ni-based catalyst seemed to be via scheme C, steam reforming to CO and H<sub>2</sub>, at low temperature. When the reformer temperature was increased, the ethanol conversion path changed to scheme A, ethanol decomposition, for Co-based catalysts and to scheme B, steam reforming to CH<sub>4</sub>, CO<sub>2</sub> and H<sub>2</sub> for Ni-based catalysts. This might be because of the decreasing activity toward methane steam reforming for both catalysts at higher temperature. In scheme C, the methane steam reforming occurs simultaneously with the ethanol decomposition reaction of Co. When the methane steam reforming activity decreased, if that catalyst has sufficient activity toward water-gas shift reaction, the ethanol conversion path will change to scheme B, if not, it will change to scheme A. Unfortunately, data at low temperature are not available for Rh-based catalysts. The only conclusion for these catalysts is that at high temperature, ethanol was converted via scheme B and it is independent of the steam/ethanol ratio.

# เนื้อหางานวิจัย

เนื้อหางานวิจัย สามารถแยกได้เป็น 3 หัวข้อหลักๆ ดังนี้

- 1. The study on the effect of ethanol concentration on Co/SiO<sub>2</sub> catalyst for the steam reforming of ethanol
- 2. Thermodynamic Calculation of the Ethanol Steam Reforming Reaction: Possibility to Produce Low-Carbon Monoxide Hydrogen Stream
- 3. Approach to equilibrium for ethanol steam reforming over cobalt, rhodium and nickel based catalysts

# The study on the effect of ethanol concentration on Co/SiO<sub>2</sub> catalyst for the steam reforming of ethanol

#### 1. Introduction

Main fuels used at present come from crude oil refinery. This energy source is limited and will be extinguish within a few decades. This necessity forces researchers to look for other alternative fuels. Fuel derived from biomass is an environmental friendly alternative. Its high availability makes it more attractive especially in agricultural countries like Thailand. The fermentation process can be incorporated to produce ethanol, which can be steam reformed to hydrogen and then further used in fuel cells. The overall process from biomass production to fuel cell operation has zero net carbon dioxide generation.

The main reaction of ethanol steam reforming is:

$$C_2H_5OH + 3H_2O \rightarrow 6H_2 + 2CO_2$$
 (1)

Other side reactions such as reverse- water gas shift generate undesired byproducts. The most important one is carbon monoxide. Carbon monoxide can poison the fuel cell electrode and inhibit the oxidation reaction taking place on the anode. Most types of fuel cells have limited CO tolerance even with more advanced anode catalysts. There are many factors that can affect carbon monoxide content in the product stream of steam reforming process. Reaction conditions, feed conditions, types of catalysts are examples. Another alternative is to incorporate a downstream process such as selective oxidation prior to fuel cell.

Metals found active to ethanol steam reforming are Pd, Rh, Ni, and Co [2-5]. These metals have been studied after being dispersed on different supports. Over a wide range of metals supported on alumina, it was found that cobalt was the most selective one at temperature around 400°C [6]. In addition, its activity can be adjusted by varying the reaction conditions [7]. The acidity of support is also another factor to consider. Ethylene production is promoted by support acidity [6]. This ethylene is the precursor of carbon that deposits on catalyst surface and makes it deactivates [6].

This study focused on the activity of Co/SiO<sub>2</sub> catalyst with varying ethanol concentrations. Co/SiO<sub>2</sub> was chosen because it was cheaper than other metals with comparable activity and its activity was expected to vary with operating conditions [7]. Effect of ethanol concentration (ethanol/water ratio) was investigated. Information from this study can be used to control the extent of fermentation process.

#### 2. Experimental

#### 2.1 Apparatus

The experimental apparatuses consist of:

- 1. Packed bed reactor, the diameter and length of reactor are 1.27 and 40 cm, respectively. The reactor is made from 316-stainless steel and assembled by SWAGELOK fitting.
- 2. Gas distributor, a portable gas distributor, the circle slate punched with distributed small holes, is used to uniformly distribute gas and to support the catalyst in the reactor.
- 3. Temperature control heater, a programmable heater controls the reactor temperature. This temperature control system is a product of Shinko Company.
- 4. Pre-heater unit, a pre-heater unit is used to vaporize the dilute ethanol solution before sending to the reactor unit. The pre-heater temperature is controlled by another programmable temperature control.
- 5. Electromagnetic dosing pump, the LMI MILTON ROY model number A962-161S is used. The maximum capacity is 2 GPH and the accuracy is 5%.
  - 6. U-tube, U-tubes are used to collect both liquid and gas samples.
- 7. Ice bath, an ice bath is used to condense the low volatile components in the reactor effluent to liquid.
- 8. Gas chromatography with TCD, the Shimadzu model 9A is used with a molecular sieve SII column to analyze  $H_2$ , CO,  $CH_4$  and  $CO_2$  composition and Porapak N to analyze the liquid sample,  $H_2O$  and  $C_2H_5OH$ . Helium, as the carrier gas, flow rate is 30 ml/min.

For Molecular sieve SII

The oven temperature was set as a function of time, which is:

0-5 min 35°C

5-9.7 min  $35^{\circ}\text{C} - 200^{\circ}\text{C}$  with ramping rate =  $35^{\circ}\text{C/min}$ 

9.7-25 min 200°C

For Porapak N

The oven temperature was set as a function of time, which is:

0-5 min 130°C

5-12 min  $130^{\circ}\text{C} - 200^{\circ}\text{C}$  with ramping rate =  $10^{\circ}\text{C/min}$ 

12-25 min 200°C

The detector temperature was set to  $240^{\circ}$ C and  $250^{\circ}$ C for front inlet and back detector, respectively. The retention times for the production gases are 1.9 sec. for H<sub>2</sub> gas, 10.4 sec. for CO, 13.4 sec. for CH<sub>4</sub>, 16.6 sec. for CO<sub>2</sub>.

- 9. Pulse ChemiSorb 2700, the PULSE CHEMISORB 2700 is used to measure the number of surface atoms or dispersion by hydrogen pulse-chemisorption technique.
- 10. X-Ray Diffraction (XRD): The JEOL analytical X-Ray Diffractometer (JEOL, JDX-3530) is used to analyze the chemical form and structure of the catalyst.
  - 11. AUTOSORB-1 supplied by Quantachrome Instruments is used to measure the

BET surface area of the silica support and the cobalt catalyst.



Figure 1: A photograph of ethanol steam reforming apparatus

# 2.2 Experimental Procedure

The experiments are divided into three main parts, which are catalyst preparation, catalyst characterization and ethanol steam reforming testing. The details of each part are shown below.

#### (a) Catalyst Preparation

For this research, 10% and 20% by weight of Co/SiO<sub>2</sub> are prepared. Co(II)nitrate hexahydrate (Co(NO<sub>3</sub>)<sub>2</sub>·6H<sub>2</sub>O) supplied by Aldrich was used as a precursor for Co metal. The preparation procedures, as shown in Figure 2, are explained step by step as follows. First, the silica gel was ground and dried at 110°C for 6 hrs. After that silica pore volume was measured by gradually dropping known volume of distilled water into silica powder until it started to get wet. Then, the same volumes of Co(NO<sub>3</sub>)<sub>2</sub>·6H<sub>2</sub>O solution with desired concentration (the calculation example is shown in Appendix A) were prepared. To deposit the metal active agent, the metal salt solutions were gradually dropped into silica power drop by drop. Next, the wetted catalyst was slowly boiled to get rid of excess water in the oven at 100°C for 12 hrs. After this step the physical appearance was powder-liked. After that, it was calcined in air at 350°C for 2 hrs. In order to have the ratio of reactor diameter to catalyst diameter about 3-6, the catalyst density was measured and appropriate amount of silica carbide was added to the catalyst. The mixture was then loaded into the reactor and reduced in the reducing step as will be mentioned in section 3.3.3.

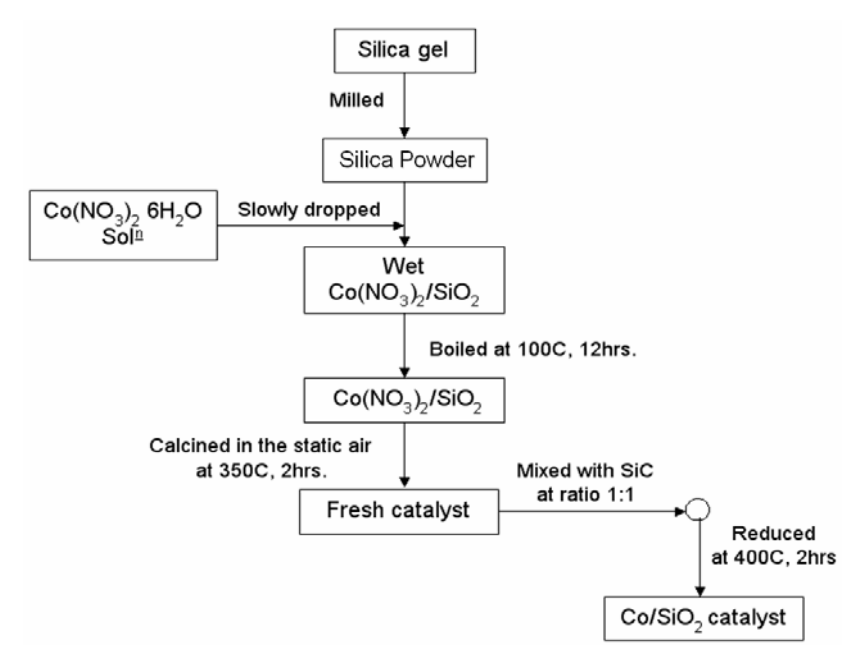


**Figure 2:** Co/SiO<sub>2</sub> catalyst preparation using incipient wetness impregnation technique.

#### (b) Catalyst Characterization

Catalyst characteristics such as cobalt dispersion, total surface area, pore size and pore volume can be determined by using two different techniques, which are H<sub>2</sub> chemisorption and N<sub>2</sub> physisorption (BET). In addition, phase of prepared catalyst was characterized by the X-ray diffraction (XRD).

#### i) N<sub>2</sub> Physisorption (BET)

The  $N_2$  physisorptions of prepared catalysts were measured by Quantachrome Instruments, AUTOSORB-1. First of all, the sample was degassed by purging helium for more than 2 hrs. After that, the sample was moved to analyzing port where it was kept at liquid nitrogen temperature (77 K). The amount of adsorbed  $N_2$  at different pressures were measured and compared with that of standard at  $P_o$  ( $P_o \sim 760\text{-}770 \text{ mmHg}$ ). After analysis, the surface area ( $m^2$ /gram of catalyst), pore volume (cc/ gram of catalyst), pore size (Å) and adsorption isotherm were reported.

#### ii) Hydrogen Chemisorption

Hydrogen chemisorption was used to determine the number of surface metal atoms and % metal dispersion. The stoichiometry of  $H_2$  chemisorption on Co metal was assumed to be 1 hydrogen atom on 1 surface Co atom (H:Co = 1:1). The analysis steps are as follow.

- 1. The pressure of inlet gases (N<sub>2</sub> and H<sub>2</sub>) was adjusted to 760 mmHg.
- 2. The 0.300 grams of catalyst sample was packed into the sample cell.

- 3. The sample tube was purged with carrier gas (N<sub>2</sub>) at 400°C to removed water.
- 4. The flow was switched to hydrogen to reduce sample at 400°C for 2 hrs.
- 5. After reduction, the sample was purged again with nitrogen to removed hydrogen inside the sample cell while it was cooled down to adsorption temperature (100°C).
- 6. Known amount of hydrogen gas was injected to the sample cell until the sample was saturated with hydrogen as reported by the value shown on the monitor.

# iii) X-Ray Diffraction (XRD)

The sample was firstly milled to smaller particle size and packed into the sample stub with even and smooth surface. Then, the packed sample stub was loaded in JEOL X-ray Diffractometer. The condition used for analyzing Co compound was set as follows:

Start angle =  $10^{\circ}$ End angle =  $100^{\circ}$ Step size = 0.02

Time per step = 0.933 min

Finally, the analysis was started

### 2.3 Reaction system

The ethanol steam reforming was carried out in a fixed-bed stainless steel reactor. Ethanol with different concentrations was fed to the preheater by the electromagnetic dosing pump (the LMI MILTON ROY model number A962-161S). Ethanol vapor and steam were flowing further through the reactor with the stream of helium. Helium was used as the carrier gas for both the reaction and the gas chromatography. The reactor outlet was connected with an ice bath to condense unreacted reactants and liquid products before the dry gas was collected in the sampling u-shape tube. The schematic diagram of this ethanol steam reforming system is shown in Fig 3.

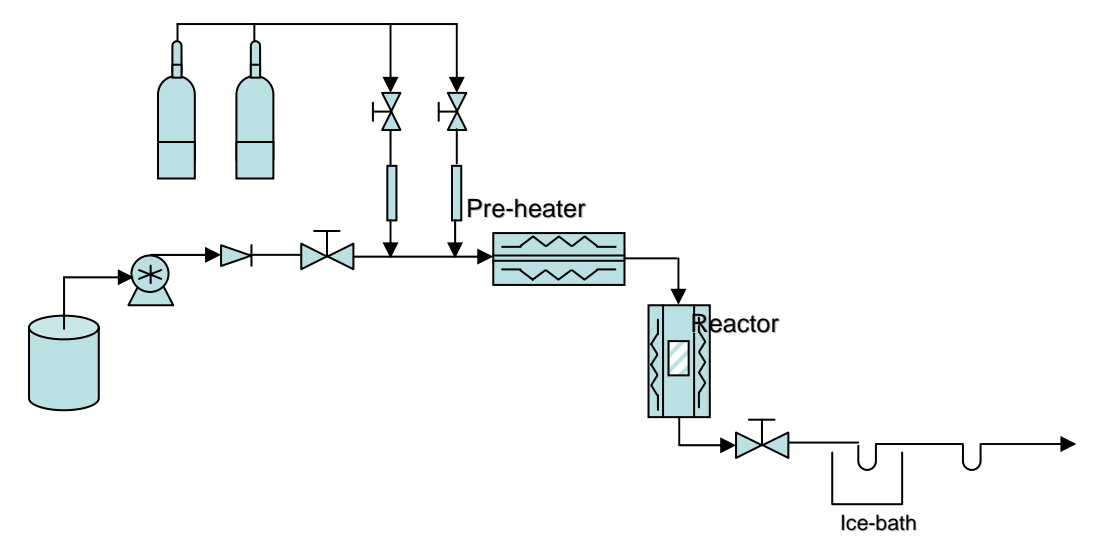


Figure 3: Schematic diagram of the ethanol steam reforming laboratory system

### 2.4 Activity measurement

Prior to the activity measurement, approximately 1.0 g of catalyst sample was reduced in situ at 400°C for 2 hrs in flowing hydrogen. The activity of the catalyst was measured under the following conditions: temperature = 450°C, total pressure = 1 atm and gas hourly space velocity (GHSV) = 12,462 cc/g·cat·hr. To study the effect of ethanol concentration, the concentration was varied from 15% by volume to 20% and 25% for the 10% Co/SiO<sub>2</sub> catalyst. Dry gas products were analyzed by TCD gas chromatography (Shimadzu model 9A) using Carbosieve SII column. For the best product separation, the oven temperature was set at 35°C for 5 min before ramping to 200°C with 35°C/min of ramping rate.

The percent ethanol conversion, hydrogen yield and carbon selectivity are defined as follows.

```
%Ethanol conversion = \frac{\text{summation of all carbon containing molecules (moles)}}{2 \times \text{amount of ethanol in feed (moles)}} \times 100\%
%Hydrogen yield = \frac{\text{amount of hydrogen generated (moles)}}{6 \times \text{amount of ethanol in feed (moles)}} \times 100\%
%Carbon selectivity = \frac{\text{amount of that species generated (moles)}}{2 \times \text{amount of ethanol converted (moles)}} \times 100\%
```

#### 3 Results and Discussion

#### 3.1 Catalyst Characterization

As shown in Table 1, results from the BET measurement showed high surface area of silica powder used as the support in this study. After cobalt was added, the total surface areas of the catalysts and catalyst pore volumes decreased as the percent metal loading increased. These indicate the possible blockage of silica pores by cobalt clusters. When considering the Co dispersion obtained from the total amount of H<sub>2</sub> chemisorption,

it is quite low for both catalysts as expected for cobalt catalysts prepared by the incipient wetness impregnation method. Results from  $H_2$  chemisorption can also be used to confirm the blockage of silica pores after calculating the Co particle size. In general, metal particle sizes can be approximated from %dispersion using the following formula [8].

$$d = \frac{108}{\%D} \tag{2}$$

where D: the dispersion (%)

d: average crystallite diameter (nm)

As shown in Table 1, the Co particle size was found to be 52.74 nm and 92.18 nm for 10%Co/SiO<sub>2</sub> 20%Co/SiO<sub>2</sub>, respectively. This large agglomeration of cobalt particles (57-92 nm) can completely block some of small mesopores of silica leading to the lower pore volume and surface area.

**Table 1** Characteristics of Co/SiO<sub>2</sub> catalysts

Catalyst	Surface area (m²/g)	Pore volume (cc/g)	Pore size (Å)	Co Dispersion (%)	Metal particle size (nm)
1)SiO <sub>2</sub> Powder	257	1.182	183.5	-	-
2) 10%Co/SiO <sub>2</sub>	237	1.014	170.7	1.8706	57.74
3) 20%Co/SiO <sub>2</sub>	199	0.829	166.8	1.1716	92.18

#### (c) X-Ray Diffraction (XRD)

Figure 4 shows the comparison between the XRD patterns of two catalysts containing different metal loadings,  $10\%\text{Co/SiO}_2$  and  $20\%\text{Co/SiO}_2$ .

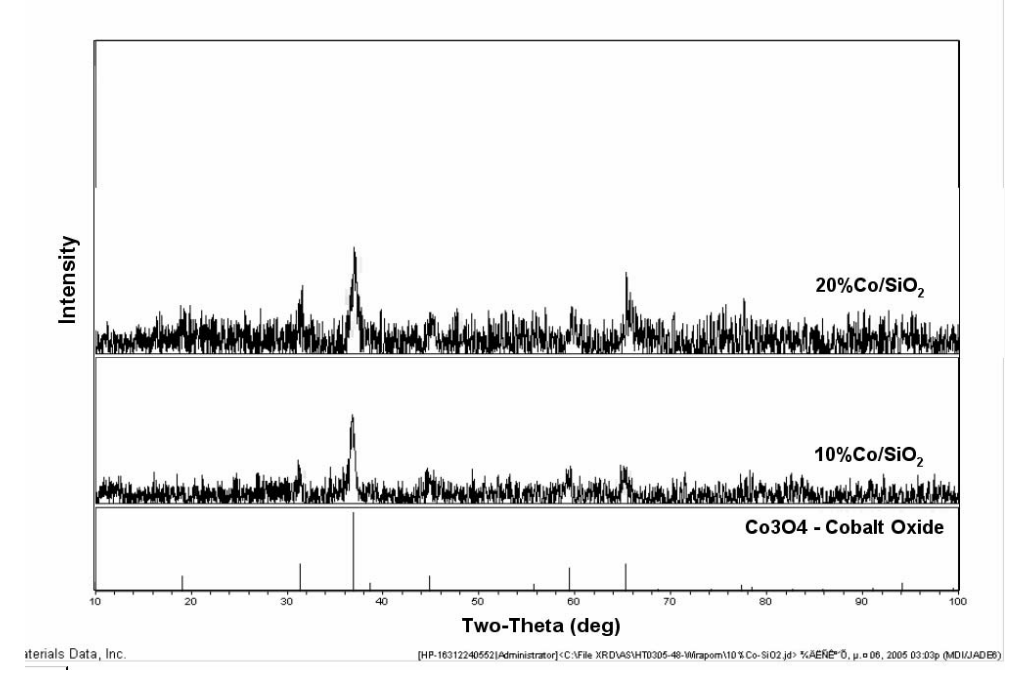


**Figure 4:** The XRD pattern of 10%Co/SiO<sub>2</sub> and 20%Co/SiO<sub>2</sub> catalysts

From Figure 4, both  $10\%\text{Co/SiO}_2$  and  $20\%\text{Co/SiO}_2$  catalysts have similar XRD patterns with the peak location matches with only cobalt oxide (Co<sub>3</sub>O<sub>4</sub>). Therefore, Co<sub>3</sub>O<sub>4</sub> is the main component in these two catalysts and calcination at  $350^{\circ}\text{C}$  for 2 hours in static air is enough to convert Co(NO<sub>3</sub>)<sub>2</sub> into Co<sub>3</sub>O<sub>4</sub>.

#### 3.2 Ethanol Steam Reforming Experiment

#### 3.2.1 Effect of ethanol concentration

In all experiments in this study, only  $H_2$ , CO,  $CO_2$ ,  $CH_4$  and He were detected in dry gas product. Ethanol conversions were in the range of 75-98% in all cases. Figure 5 shows the variation of the composition in dry gas product with ethanol concentration over  $10\%Co/SiO_2$  catalyst. When the ethanol concentration increased, the percentage of all components in the product increased. In this study, the amount of CO generated was approximately 10-20% of hydrogen production, which is consistent with other works on  $Co/SiO_2$  catalyst reported by Batista et al. [9] and Kaddouri and Mozzozhia [10] but at higher ethanol concentrations and lower temperature. In addition, the amount of  $CH_4$  and CO are approximately the same, which is also consistent with the results reported by Batista et al. [9] and Kaddouri and Mozzozhia [10], suggesting that the decomposition reaction of ethanol ( $C_2H_5OH \rightarrow CH_4+CO+H_2$ ) be responsible for the formation of both CO and  $CH_4$ . When comparing with reported work on  $8\%Co/SiO_2$  catalyst [10], at the same reaction temperature,  $\%CO_2$  in this work is quite high this might be resulted from the higher oxidation capacity of  $10\%Co/SiO_2$  to convert CO into  $CO_2$ . It is confirmed by the other work reported by Batista et al. [9] that the amount of  $CO_2$  in the effluent gas

increases and the amount of CO decreases when the metal loading was increased from 8 to 18% for Co/SiO<sub>2</sub> catalyst. See further discussion in section 3.2.2.

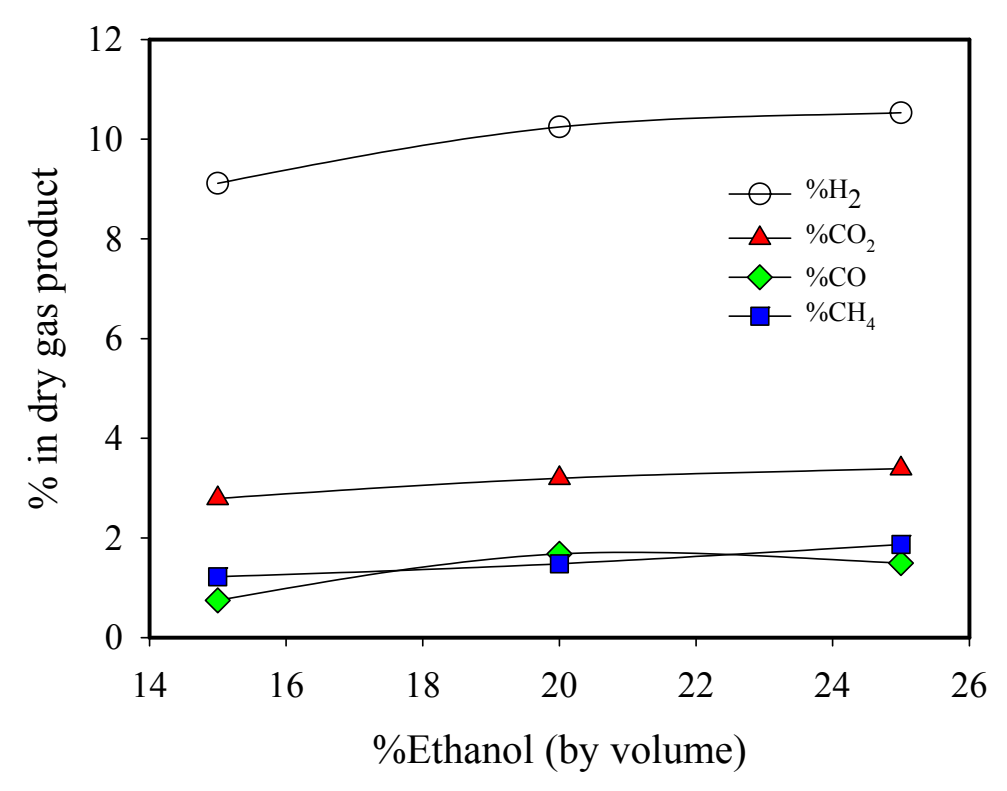


**Figure 5:** The variation of the percentage in dry gas product with %ethanol in feed (balance He).

Although the amount of hydrogen in dry gas product increased with %ethanol, when considering the hydrogen yield as defined in section 2.4, it slightly decreased as shown in Fig.6. From this point forward, in all figures, %E stands for %ethanol by volume, and %Co stands for %cobalt loading in silica-supported catalysts. Although, the time-on-stream behavior of the hydrogen yields at different ethanol concentrations and %Co loadings was quite fluctuated, it is clearly seen in Fig. 6 that the hydrogen yield decreased with ethanol concentration and increased with %Co loading. The decrease in hydrogen yield when increasing ethanol concentration might be due to the higher degree of coke formation at higher ethanol concentrations. The comparison between two metal loadings, 10 and 20% cobalt, at the same ethanol concentration showed a significant increase in hydrogen yield when increasing metal loading. Steady-state hydrogen yields were 57% and 84% for 10% and 20% cobalt loading, respectively. This result was not surprised since the 20% Co/SiO<sub>2</sub> catalyst has more surface metal atoms compared to the 10% Co/SiO<sub>2</sub> catalyst. The decrease of hydrogen yield with ethanol concentration was also observed for the ethanol steam reforming on other catalysts such as what was reported by Laosiripojana and Assabumrungrat [11] over Ni/Al<sub>2</sub>O<sub>3</sub> and Rh/Al<sub>2</sub>O<sub>3</sub>

catalysts. When plotting the selectivities towards H<sub>2</sub>, CO<sub>2</sub>, CO and CH<sub>4</sub> with ethanol concentration, shown in Fig. 7, it is obvious that the selectivities towards H<sub>2</sub> and CO<sub>2</sub> decreased with ethanol concentration while that of methane increased and that of CO showed a maximum at 20% ethanol. The results obtained over Co/SiO<sub>2</sub> in this study were similar to the results reported when using Pd/Al<sub>2</sub>O<sub>3</sub> [3], Ni/Al<sub>2</sub>O<sub>3</sub> [4], Rh/Al<sub>2</sub>O<sub>3</sub> [12] and Ni/Cu [13] catalysts. In addition, the effect of H<sub>2</sub>O/EtOH ratio was less observable when H<sub>2</sub>O/EtOH ratio is getting larger.

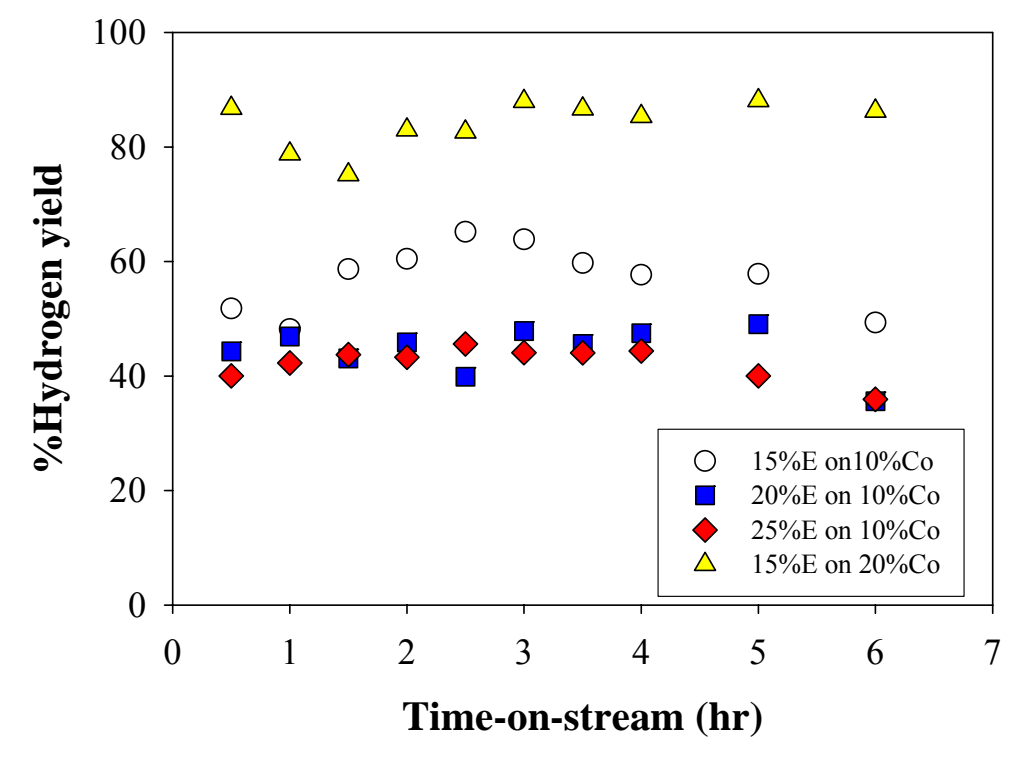


**Figure 6:** The variation of hydrogen yield with ethanol concentrations on 10%Co/SiO<sub>2</sub> catalyst and at 15% ethanol concentration on 20% Co/SiO<sub>2</sub> catalyst.

If assuming that the number of active atoms equal the number of surface atoms as measured by  $H_2$  chemisorption, the specific rate in term of turnover frequency can be calculated. As shown in Fig. 8, the turnover frequency increases when increasing the concentration of ethanol from 15% to 20% and 25% by volume. It suggests that at low ethanol concentration, Co surface atoms are not fully utilized. Lots of vacant surface atoms are still available for reaction. The specific reaction per gram of catalyst is thus dependent on the probability of surface atom contacting with ethanol molecule. When following the turnover frequency with time-on-stream, it can be seen that the turnover frequency does not change much. The deactivation of this catalyst is not observed during 6 hr time-on-stream.

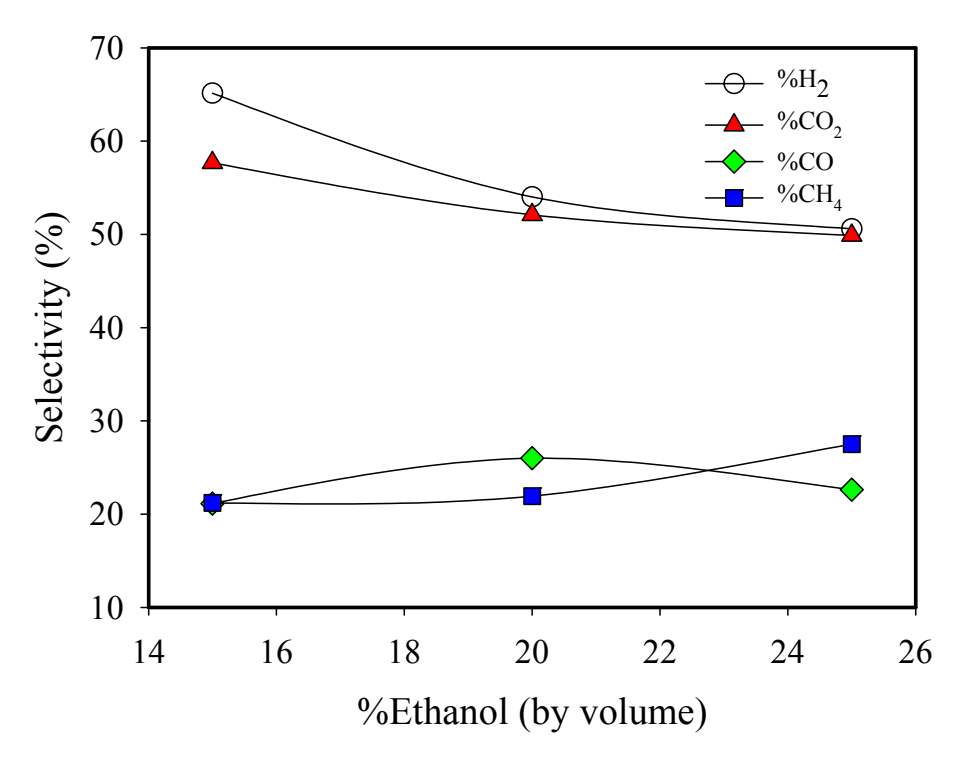


**Figure 7:** Effect of %ethanol (by volume) on the selectivity of H<sub>2</sub>, CO<sub>2</sub>, CO and CH<sub>4</sub> obtained over 10%Co/SiO<sub>2</sub> catalyst at 450°C.

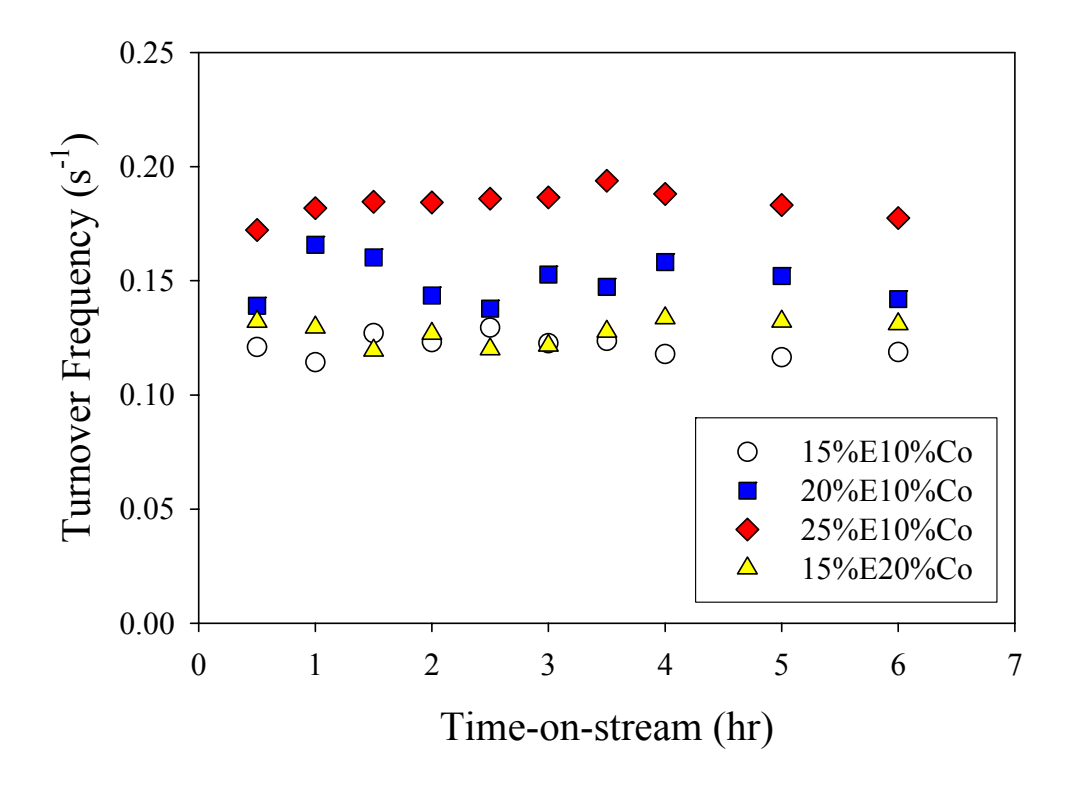


**Figure 8:** Time-on-stream behavior of the turnover frequency of 10%Co/SiO<sub>2</sub> catalyst at varying ethanol concentration and that of 20% Co/SiO<sub>2</sub> at 15% ethanol by volume at 450°C.

# 3.2.2 Effect of metal loading

The effects of %Co loading on the selectivity of H<sub>2</sub>, CO<sub>2</sub>, CO and CH<sub>4</sub>, and %ethanol conversion at 15% ethanol (by volume) are shown in Fig. 9. Since the reaction was operated at total conversion, the effect of %Co loading on ethanol conversion was only slightly even though %Co loading was doubled. From this figure, it is clearly seen that the selectivities towards H<sub>2</sub> and CO<sub>2</sub> were improved when using higher Co loading. The decrease in the selectivity towards CO and CH<sub>4</sub> accompanied by an increase of the CO<sub>2</sub> selectivity implied that the rate of water-gas-shift reaction increases, and the rate of methanation, the undesired reaction, decreases at higher Co loading. These results are consistent with what was reported by Batista et al. [9] that smaller amount of methane was produced for the catalyst at higher Co loading. Although the increase in H<sub>2</sub> production yield when using 20%Co/SiO<sub>2</sub> is not twice that from 10% Co/SiO<sub>2</sub>, it shows the advantage in using higher Co loading in terms of the quality of the product gas.

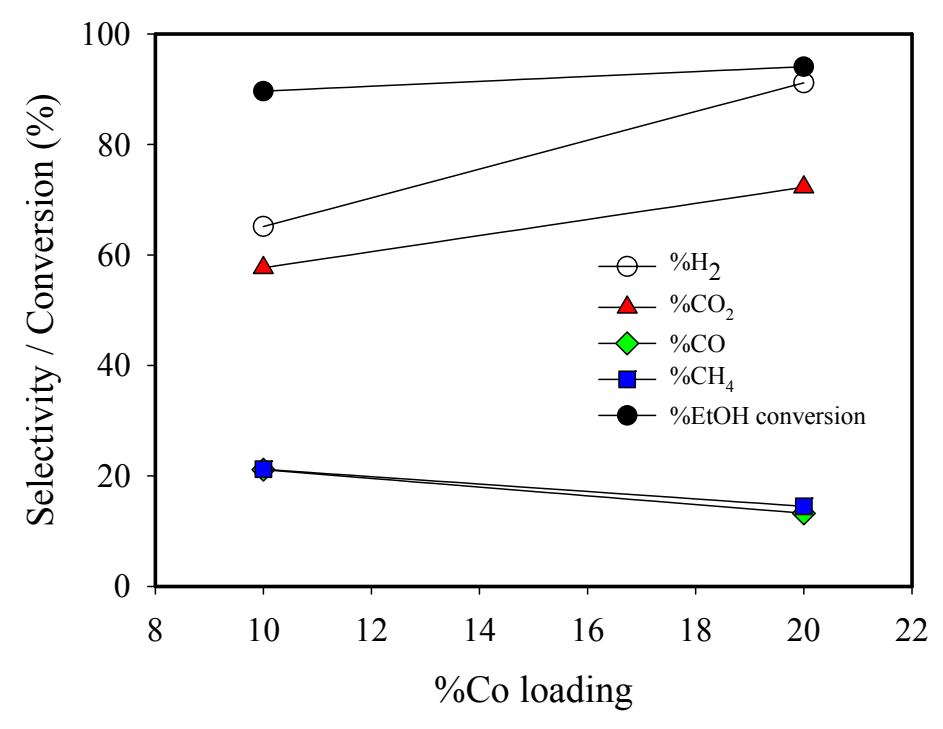


**Figure 9:** Effect of %Co loading on the selectivity of H<sub>2</sub>, CO<sub>2</sub>, CO and CH<sub>4</sub>, and %ethanol conversion obtained at 15% ethanol (by volume) and 450°C.

Turnover frequency may differ significantly (factor of 2-1000) among catalysts of the same type because of (1) differences in surface structure in a structure sensitive reaction, (2) varying degree of metal-support or metal-promoter effects, and (3) differences in surface composition in a series of bimetallic or multi-metallic catalyst [8]. For the catalysts in this study, both 10% and 20%  $Co/SiO_2$  catalysts exhibit the same turnover frequency (Fig.8) , which means that the intrinsic activity of both catalysts are

approximately the same despite the different in metal particle size (Table 1). It implies that the steam reforming of ethanol is a structural insensitive reaction at the condition studied in this work.

#### 3. 3 Catalyst Deactivation

After 6 hours time-on-stream, the used catalyst was taken out from the reactor and characterized by using the BET technique. The results were then compared to the fresh catalyst as shown in Table 2. As can be seen in Table 2, the total surface of all catalysts after being used in the reaction remained approximately the same even though there was large amount of steam in the reactor. Although sintering can easily occur at this condition, the BET results show no reduction in the surface area of the support. However, pore volume and pore size of both catalysts reduced slightly probably by slight coke formation inside the mesopores.

**Table 2** The BET results of catalysts after 6 hr time-on-stream compared to fresh catalysts.

Catalyst	% Ethanol	Surface area (m <sup>2</sup> /g)	Pore volume (cc/g)	Pore size (Å)
		Fresh/ used	Fresh/ used	Fresh/ used
10%Co/SiO <sub>2</sub>	15	237/250	1.014/0.890	170.7/141.8
	20	237/237	1.014/0.922	170.7/155.4
	25	237/228	1.014/0.884	170.7/154.5
20%Co/SiO <sub>2</sub>	15	199/214	0.829/0.790	166.8/146.3

#### 4. Conclusions

Low metal dispersion was observed for the 10% and 20% Co/SiO<sub>2</sub> catalysts prepared in study. It resulted in large agglomeration of Co particle and slightly lower BET surface area, pore volume and pore size. For 10% Co/SiO<sub>2</sub> catalyst, although the amount of all components in the product gas increased when increasing ethanol concentration, it decreased in term of hydrogen yield. It implied that less ethanol in feed was converted to hydrogen when increasing the concentration of ethanol. It is confirmed by the selectivity toward hydrogen that it was decreased and accompanied by the increase in CH<sub>4</sub> selectivity with ethanol concentration. Although the degree of catalyst utilization of the 10% Co/SiO<sub>2</sub> catalyst can be enhanced by increasing ethanol concentration, 15% ethanol by volume seems to be the best concentration in term of the quality of product gas to be further used in fuel cell after pretreatment. Thus, bio-ethanol from the fermentation of biomass can be directly used to produce hydrogen without distillation step. The result on the effect of metal loading showed that high metal loading is preferable in term of hydrogen yield and the quality of product gas. However, it must be traded off with the

price of metal being using to prepare the catalyst. In addition, despite a large amount of steam in the reactor, deactivation from support sintering was not observed during the entire reaction time for all cases in this study.

# Thermodynamic Calculation of the Ethanol Steam Reforming Reaction: Possibility to Produce Low-Carbon Monoxide Hydrogen Stream

#### 1. Introduction

The ethanol steam reforming of ethanol is important reaction to generate hydrogen stream to be used as fuel cell feed. Although, in general, the main reaction of ethanol steam reforming can be written as:

$$C_2H_5OH + 3H_2O \rightarrow 6H_2 + 2CO_2$$
 (1),

there are actually many reactions occurring in the reformer including ethanol decomposition, water-gas-shift and steam reforming of methane. These reactions generate undesired products, especially carbon monoxide, which can poison fuel cell electrode even only a few ppm is present. The composition of the product gas from reformer, thus, depends on the activity and selectivity of the catalyst towards these reactions. However, if the reformer is operated at equilibrium, the composition will be the same for all catalysts at a given temperature and feed composition. The possibility to produce hydrogen stream with suitable purity can be anticipated by incorporating the information at equilibrium.

In this study, the composition at equilibrium was determined using Lagrange's undetermined multipliers. The results were compared with the method proposed by Mas et al. [1], which provided the equilibrium conversion of each reaction for each proposed mechanism. From the comparison, the influence of catalytic activity on the product gas composition can be evaluated. In addition, the composition of hydrogen stream after being treated in Low-temperature shift reactor was also investigated for the possibility to be used in fuel cells.

#### 2. Experimental

2.1 Equilibrium calculation using the method of total Gibbs energy minimization

At specified temperature and pressure, the set of  $\{n_i\}$  which minimize  $G^t$  can be determined based on the method of Lagrange's undetermined multipliers [14]. For the ethanol steam reforming reaction, the equilibrium amount of ethanol, hydrogen, carbon dioxide, carbon monoxide methane and water are our interest. With  $\lambda_k$  as the Lagrange multiplier for each element and r as the steam/ethanol ratio, a set of non-linear equations consists of the following;

C<sub>2</sub>H<sub>5</sub>OH: 
$$\frac{\Delta G_{EtOH}^{o}(T)}{RT} + \ln(\frac{n_{EtOH}}{n}) + \frac{2\lambda_{C}}{RT} + \frac{6\lambda_{H}}{RT} + \frac{\lambda_{O}}{RT} = 0$$
 (2)

CH<sub>4</sub>: 
$$\frac{\Delta G_{CH4}^{o}(T)}{RT} + \ln(\frac{n_{CH4}}{n}) + \frac{\lambda_C}{RT} + \frac{4\lambda_H}{RT} = 0$$
 (3)

H<sub>2</sub>O: 
$$\frac{\Delta G_{H2O}^{o}(T)}{RT} + \ln(\frac{n_{H2O}}{R}) + \frac{2\lambda_H}{RT} + \frac{\lambda_O}{RT} = 0$$
 (4)

CO: 
$$\frac{\Delta G_{CO}^{o}(T)}{RT} + \ln(\frac{n_{CO}}{n}) + \frac{\lambda_{C}}{RT} + \frac{\lambda_{O}}{RT} = 0$$
 (5)

$$CO_2: \frac{\Delta G_{CO2}^o(T)}{RT} + \ln(\frac{n_{CO2}}{n}) + \frac{\lambda_C}{RT} + \frac{2\lambda_O}{RT} = 0$$
 (6)

H<sub>2</sub>: 
$$\frac{\Delta G_{H2}^{o}(T)}{RT} + \ln(\frac{n_{H2}}{n}) + \frac{2\lambda_{H}}{RT} = 0$$
 (7)

By assuming that feed consists of 1 mole of ethanol and r moles of water, three atomic balance equations can be written as:

C: 
$$n_{CH4} + n_{CO} + n_{CO2} + 2n_{EtOH} = 2$$
 (8)

H: 
$$4n_{CH4} + 2n_{H2O} + 2n_{H2} + 6n_{FtOH} = 6 + 2r$$
 (9)

O: 
$$n_{H2O} + n_{CO} + 2n_{CO2} + n_{FtOH} = 1 + r$$
 (10)

The total number of moles in the system is

$$n = n_{CH4} + n_{H2O} + n_{CO} + n_{CO2} + n_{H2} + n_{EtOH}$$
 (11)

The Gibbs energies of formation of all components at temperature from 523 K to 1173 K were calculated and shown in Figure 1.

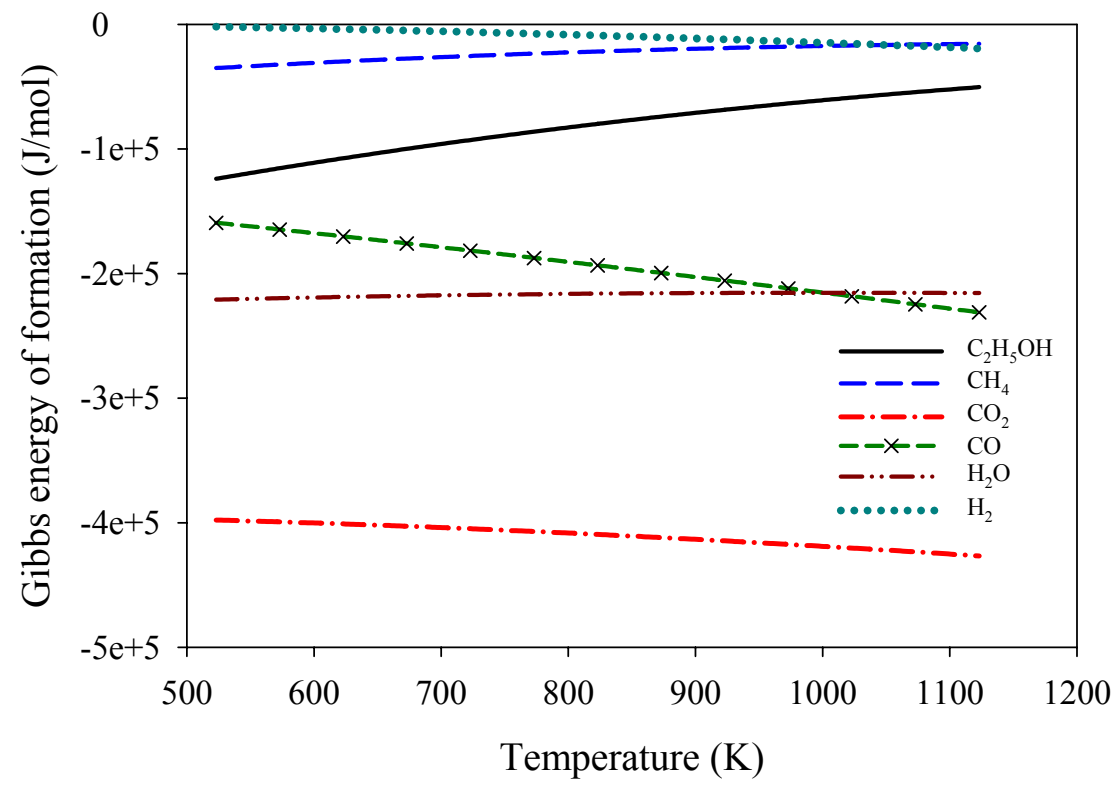


**Figure 1:** The standard Gibbs energies of formation of C<sub>2</sub>H<sub>5</sub>OH, CH<sub>4</sub>, CO<sub>2</sub>, CO, H<sub>2</sub>O and H<sub>2</sub> as functions of temperature.

Set of non-linear equations and explicit equations was then used to determine the equilibrium composition when varying reaction temperatures from 523 K to 1173 K and steam/ethanol ratios from 3 to 9 and 18.

# 2.2 Equilibrium calculation using equilibrium constant approach

Another approach to determine the equilibrium composition of ethanol steam reforming product is to follow the method explained by Mas et al. [1]. Since there are only three independent atomic species, set of three independent reactions were used in the calculation. Two different schemes of ethanol conversion were proposed in the work reported by Comas, et al. and Mas et al. [1, 4] and the other is proposed in this study for comparison. In the first scheme, ethanol was decomposed to 1 mole each of methane, carbon monoxide and hydrogen  $(C_2H_5OH = CH_4+CO+H_2)$ . In the other two schemes, ethanol was reformed by one mole of water to form 1 mole of methane, 1 mole of carbon dioxide and 2 moles of hydrogen (C<sub>2</sub>H<sub>5</sub>OH + H<sub>2</sub>O= CH<sub>4</sub>+CO<sub>2</sub>+2H<sub>2</sub>) for scheme 2, and to 2 moles of carbon monoxide and 4 moles of hydrogen (C<sub>2</sub>H<sub>5</sub>OH + H<sub>2</sub>O= 2CO+4H<sub>2</sub>) for scheme 3. The other two reactions occurred sequentially during the steam reforming process, which were used in the equilibrium calculation in all schemes were water-gas shift reaction (CO +  $H_2O = CO_2 + H_2$ ) and the steam reforming of methane (CH<sub>4</sub> +  $H_2O =$ CO + 3H<sub>2</sub>). The equilibrium conversion of ethanol was close to 100% at all temperatures above 500 K [1]. Therefore, total conversion of ethanol was assumed. Assuming ideal gas at this condition, set of non-linear equations can be solved by using Newton method in the Polymath program. The number of moles of all components can be written as functions of WGS conversion ( $X_{WGS}$ ) and SRM conversion ( $X_{SRM}$ ) as follows.

	Scheme A	Scheme B	Scheme C
Hydrogen	$1+X_{WGS}+3X_{SRM}$	$2+X_{WGS}+3X_{SRM}$	$4+X_{WGS}+3X_{SRM}$
Carbon dioxide	$X_{ m WGS}$	$1+X_{WGS}$	$X_{ m WGS}$
Carbon monoxide	1- $X_{WGS}$ + $X_{SRM}$	$-X_{WGS} + X_{SRM}$	$2-X_{WGS} + X_{SRM}$
Methane	$1-X_{SRM}$	$1-X_{SRM}$	- $X_{SRM}$
Water	r- X <sub>WGS</sub> - X <sub>SRM</sub>	r-1- X <sub>WGS</sub> - X <sub>SRM</sub>	r-1- X <sub>WGS</sub> - X <sub>SRM</sub>

 $X_{WGS}$ ,  $X_{SRM}$  stand for equilibrium conversion of water-gas shift and methane steam reforming reactions, respectively. After the equilibrium constant for each reaction at the temperature of interest was calculated (as shown in Fig. 2), it was inserted into the non-linear equations and set of equations was then solved for  $X_{WGS}$  and  $X_{SRM}$ .

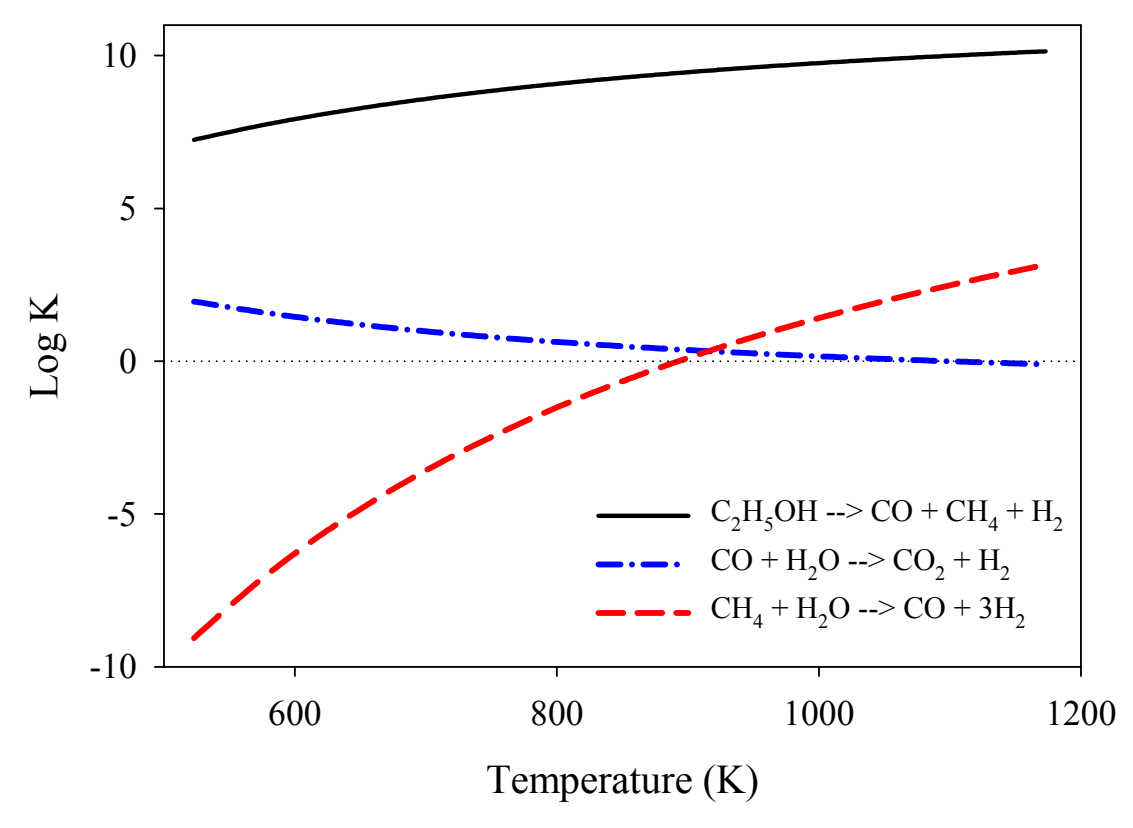


**Figure 2**: Equilibrium constants for ethanol decomposition reaction, water-gas-shift reaction and methane steam reforming reaction as a function of temperature.

#### 3. Results & Discussion

#### 3.1 Equilibrium composition

After the result was generated, it can be used to confirm the complete conversion of ethanol as previously assumed in section 2.2. It is worth noting that the mole fraction of ethanol in the product is less than  $10^{-11}$  in all cases, which confirms the complete conversion of ethanol assuming in section 2.2. Compositions of dry gas products at different temperatures and steam/ethanol ratios are shown in Fig. 3. It is not surprising that both approaches provided the same results. In addition, all schemes in the equilibrium constant approach gave the same equilibrium amounts of products. However, the equilibrium conversions for water-gas-shift and methane steam reforming are different from one scheme to another as shown in Fig. 4. As can be clearly seen in Fig 3, high temperatures of up to  $\sim 900$  K are preferable for high hydrogen content. However, at these high temperatures, high amount of carbon monoxide is also produced. Although the amount of hydrogen can be increased and the amount of carbon monoxide can be decreased by increasing the steam/ethanol ratio, the amount of carbon monoxide in product gas is still too high ( $\sim 3.2\%$  at 873 K, r=18). Thus, further treatment is required.

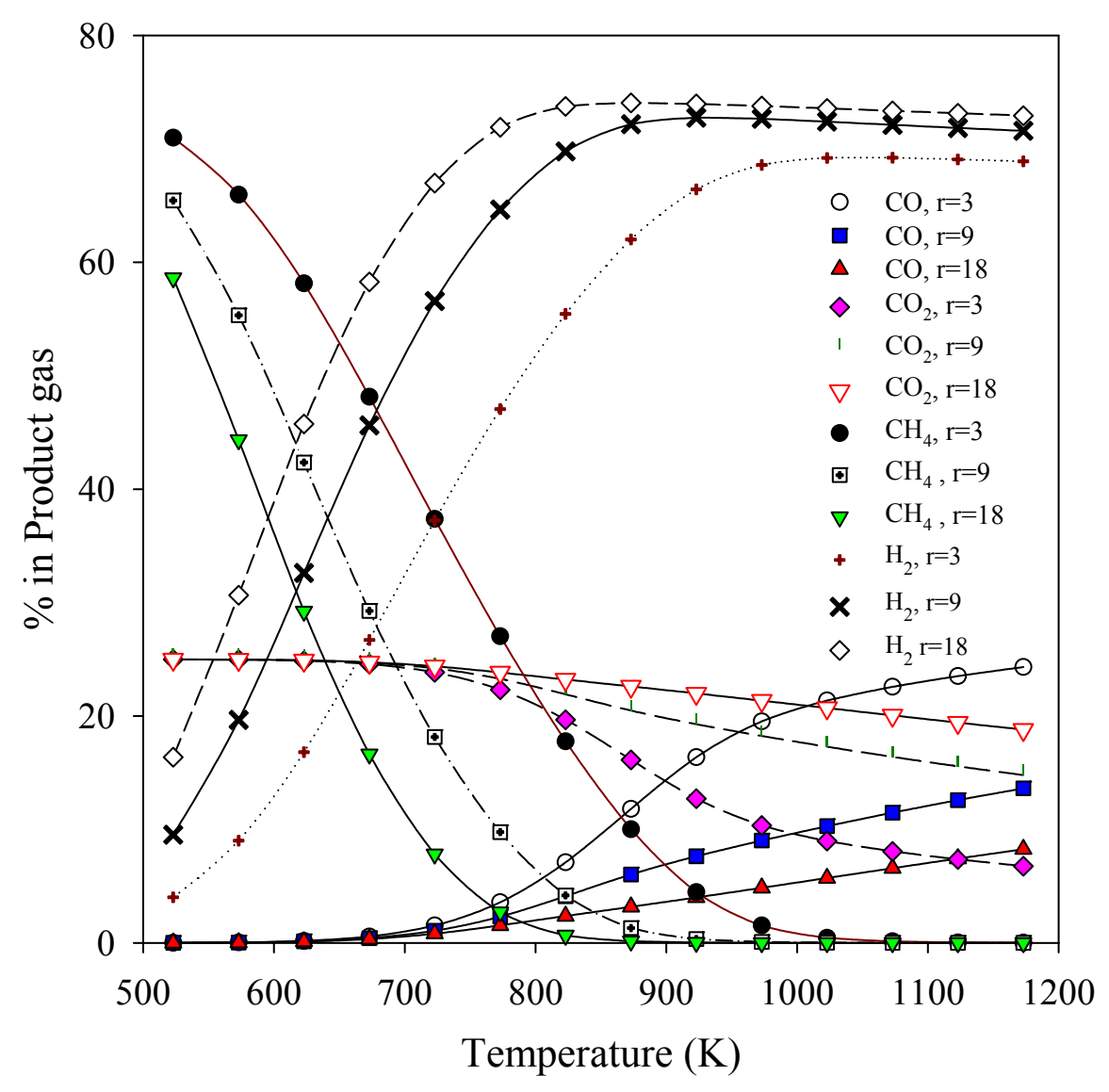


**Figure 3:** The equilibrium composition in dry gas product when varying steam/ethanol ratios and temperatures.

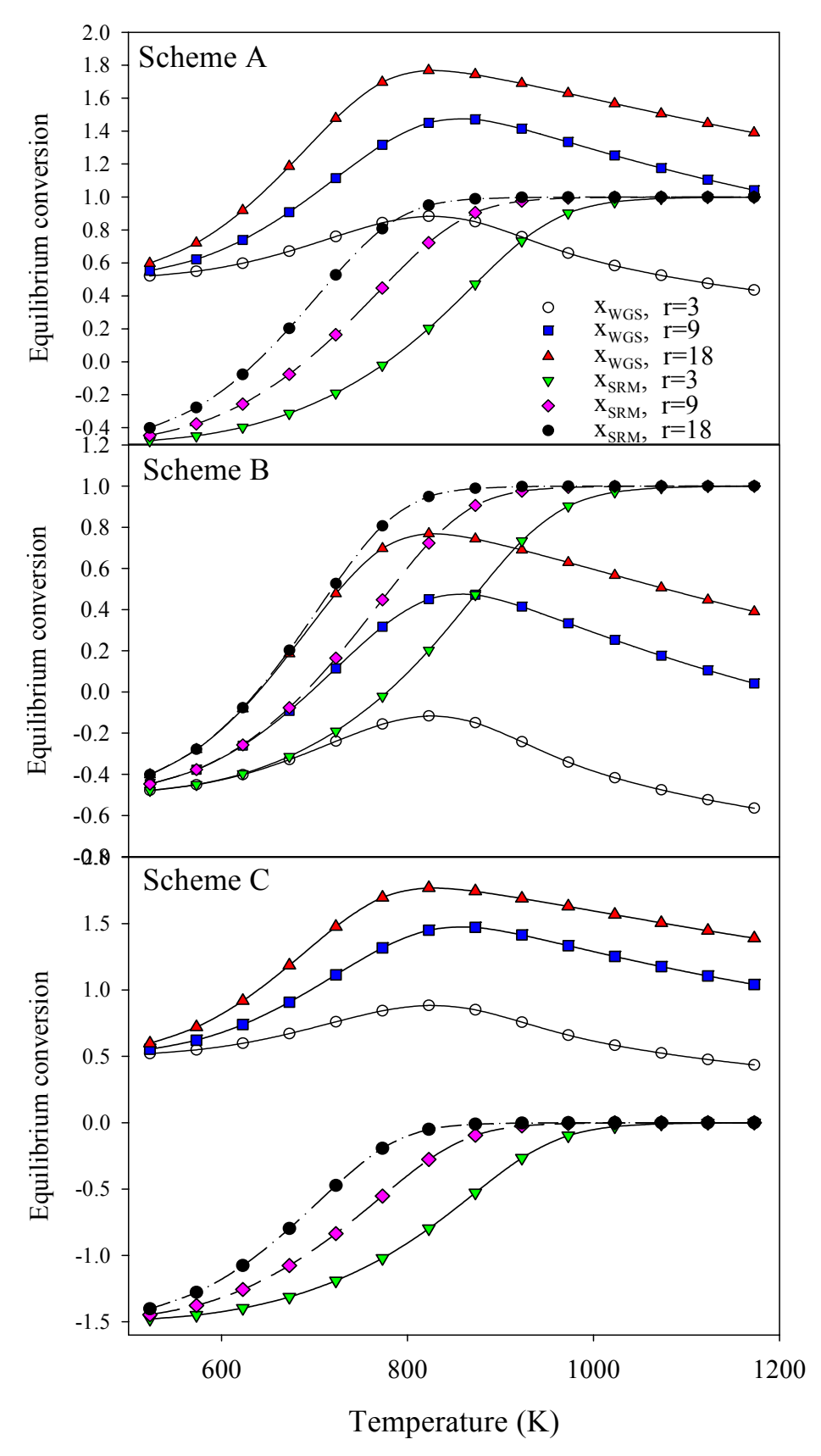


**Figure 4:** Equilibrium conversions for water-gas-shift reaction and methane steam reforming reaction from the calculation using scheme A, B and C.

The equilibrium calculation results in terms of equilibrium conversions for watergas-shift ( $X_{WGS}$ ) and methane steam reforming ( $X_{SRM}$ ) reactions are shown in Fig. 4. Similar shape of both equilibrium conversions was obtained in all schemes despite their different starting and end points. Since water-gas shift reaction is exothermic, its equilibrium conversions reach a maximum at around 810-830 K before starting to decrease. In all schemes, increasing steam/ethanol ratio results in the increase in both water-gas-shift and methane steam reforming conversions. With different ethanol conversion paths, the extent of water-gas shift and methane steam reforming reactions were adjusted until reaching the product composition that provides the lowest Gibbs free energy of the system at that particular temperature. In the real operation, which is far from equilibrium, one would expect that the composition of the product gas would depend on the activity of the catalyst toward WGS and SRM reactions.

#### 3.2 Role of catalysts

During the steam reforming of ethanol, catalyst would play an important role on the rate of approaching equilibrium. If the steam reforming catalyst is not active for any one of the three reactions (ethanol conversion, WGS or SRM), operating at equilibrium condition is impossible and the product composition will be different from the equilibrium values as shown in Fig. 3. For example, if the catalyst is active for only ethanol decomposition and steam reforming of methane, water-gas-shift reaction would be suppressed and carbon dioxide could not be generated. The product composition at equilibrium in this case calculated from the minimum Gibbs approach would be similar to Fig. 5.

It can be seen that, for this case, temperature and steam/ethanol ratio do not have an effect on carbon monoxide content. In addition, steam/ethanol ratio has less effect on hydrogen and methane contents compared to the condition with three reactions occurring (Fig. 3). When comparing with Fig.3, at the same temperature and steam/ethanol ratio, using catalyst with WGS activity provides more hydrogen and less methane. Temperatures above 800 K are still necessary for high H<sub>2</sub> selectivity.

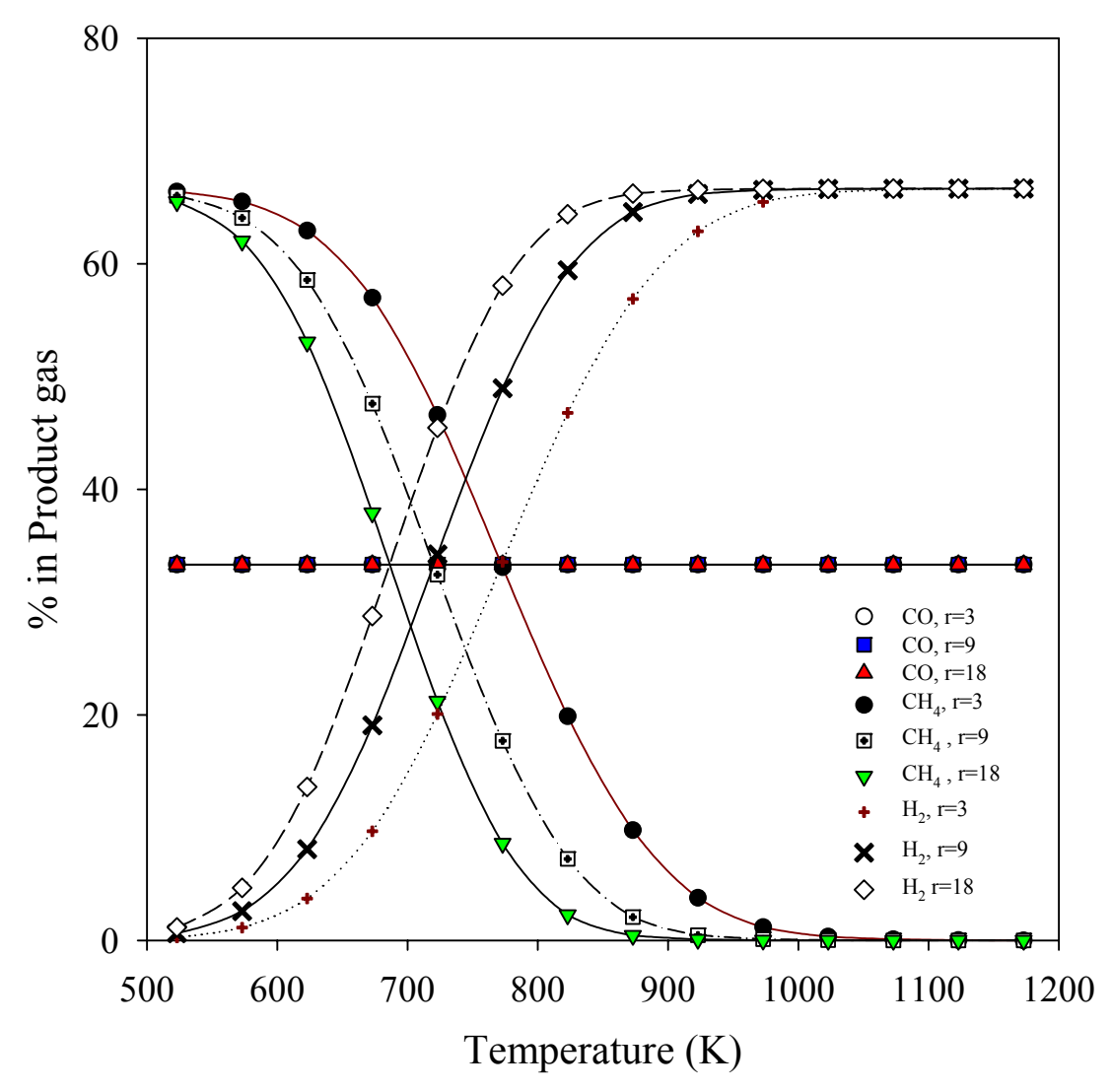


**Figure 5:** The equilibrium composition in dry gas product when varying steam/ethanol ratios and temperatures if the steam reforming catalyst is not active for water-gas-shift reaction.

#### 3.3 Low-temperature shift reactor

Since the ideal hydrogen stream to be used in fuel cell is to have very small CO content, for example, less than 1% for solid oxide fuel cell and less than 100 ppm for PEM fuel cell, further treatments of reformate gas is necessary. Such treatments include Low-temperature shift (LTS) reactor to convert CO to CO<sub>2</sub> at temperature around 200°C. In this part of study, the equilibrium composition of reformate obtained in section 3.1 was further analyzed for its equilibrium composition in the LTS. An important assumption is that the LTS catalyst is not active for other reactions especially the steam reforming of methane. The plot of the composition in product stream after being treated in LTS at 200°C is shown in Fig. 6, with the x-axis as the temperature in reformer.

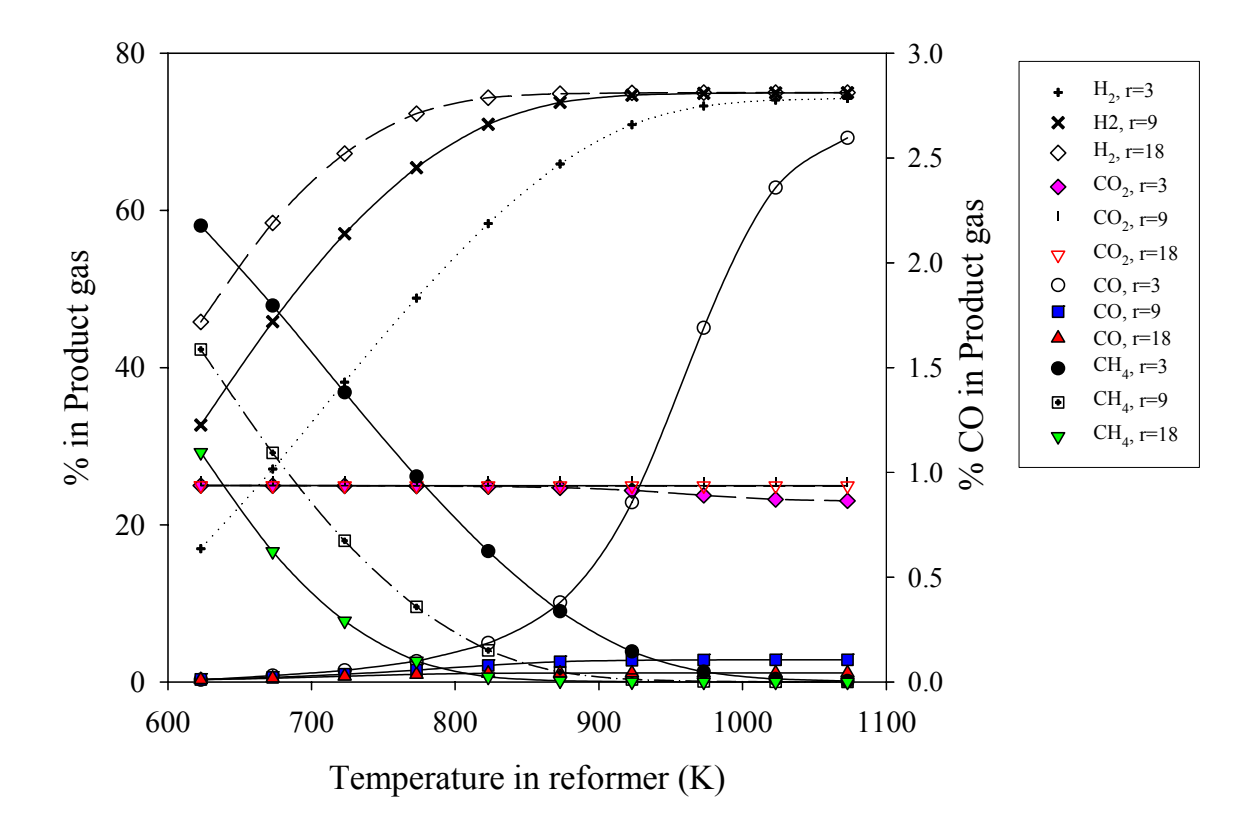


**Figure 6.** Equilibrium composition in Low-temperature shift reactor at 200°C using product gas from reformer at different conditions as feed.

It is clearly seen in Fig. 6 that at low steam/ethanol ratio (r=3), the operating temperature in reformer cannot be higher than ~950 K to be used in solid oxide fuel cells without further treatment. At high steam/ethanol ratio, the temperature can go up to 1073 K without CO problem. However, to be used in PEM fuel cells, reformer temperature has to be lower than 623 K at r=18, but low hydrogen yield would be obtained, which is not economically attractive. Therefore, from this thermodynamic analysis, it can be concluded that only steam reformer and LTS treatment are not suitable to produce hydrogen stream to be used with PEM fuel cell and another treatment such as selective CO oxidation is necessary.

#### 3.4 Selective CO oxidation reactor

Since the equilibrium conversion of CO oxidation is close to 100% at normal operating temperatures, the activity and selectivity of selective oxidation catalysts will play an important role on the reaction rate and CO<sub>2</sub> selectivity. Many catalysts were found suitable for this purpose such as Pt-based, Au-based, and Rh-based catalysts. Effects of promoters, supports and preparation methods have been studied to improve catalytic activity and selectivity of the catalysts especially at low temperature to be

compatible with fuel cell operation.

The selective oxidation of CO in the presence of hydrogen was first studied using a Pt/alumina catalyst in 1963 [15]. In 1997, Igarashi et al. [16] investigated the effect of the support on the selectivity of Pt catalysts for CO oxidation and found that Pt supported on mordenite showed the highest selectivity (~25% at 150°C), as well as high conversion of CO during oxidation at low oxygen concentration. The study by Kahlich et al. [17] in 1997 used the preferential oxidation process (PROX) to determine the optimum temperature, the reaction order, and the apparent activation energy of CO oxidation on Pt/Al<sub>2</sub>O<sub>3</sub>. It is found that the optimum temperature is 200°C at 1 bar and the reaction orders are -0.4 for CO and +0.8 for O<sub>2</sub> for temperatures between 150°C and 250°C. The CO<sub>2</sub> selectivity for this catalyst was only 25% at 100°C. Later in the year 2000, Manasilp and Gulari [18] studied the selectivity of a 2% Pt/alumina sol-gel catalyst in a mixed feed stream including CO<sub>2</sub> and water. The selectivity toward CO<sub>2</sub> was found to be between 40-60% despite the different in feed conditions. The effect of promoter on Pt catalyst has been widely studied using Fe promoter. In 2000, Korotkikh and Farrauto [19] reported on the effect of a promoter oxide on the activity of 5 wt% Pt/alumina. With a base metal oxide promoter, the CO conversion is significantly increased from 13.2 to 68% at 90°C and a molar ratio of  $O_2/CO = 0.5$  without affecting the selectivity (78%). Later, in the year 2003, Watanabe et. al [20] proposed Pt-Fe/mordenite catalysts, which have extremely high activity, selectivity (100%) and stability at 80-150°C at high GHSV.

A supported gold catalyst has been one of the most interesting catalysts studied recently, displaying higher activity and selectivity than Pt catalysts at low temperature. In 1999, Grunwaldt et al. [21] examined the extent of support interaction with 2 nm mean particle size gold clusters used to catalyze CO oxidation. They found that gold particles are different on different supports and had different catalyst activities. The kinetics of selective CO oxidation over Au/α-Fe<sub>2</sub>O<sub>3</sub> was investigated by Kahlich et al. in 1999 [22]. At 80°C, the reaction orders were 0.55 and 0.27 with respect to CO and O<sub>2</sub>, respectively, and the selectivity reached 75% at high CO partial pressure (P<sub>CO</sub>) but decreased significantly when  $P_{CO}$  decreased (at  $O_2/CO = 1$ ). Bethke and Kung [23] investigated the selective oxidation of CO over a series of Au/γ-Al<sub>2</sub>O<sub>3</sub> catalysts. Without magnesium citrate in the preparation solution, the average Au particle size seemed to be larger than the size obtained with Mg citrate present, resulting in a less active catalyst. At 100°C, about 50% (at  $O_2/CO = 0.5$ ) selectivity was obtained over the more selective catalysts. The optimal average gold crystallite size was reported to be around 5-10 nm. In 2001, Grisel and Nieuwenhuys [24] found that MgO and MnO<sub>x</sub> improve the CO oxidation activity and CO<sub>2</sub> selectivity on Au/Al<sub>2</sub>O<sub>3</sub> by stabilizing small gold particles. The CO<sub>2</sub> selectivity at  $100^{\circ}$ C and lower for these catalysts was higher than 90% at  $O_2/CO = 0.5$ . Recently, Avgouropoulos et al. [25] has shown that the activity and selectivity of ceriasupported Au catalysts depends strongly on the preparation method. At 100°C, the selectivity of Au/CeO<sub>2</sub> catalysts was approximately 35-60% for the catalyst prepared by the deposition-precipitation and modified deposition-precipitation methods, respectively.

Other metal-based catalysts have also been tested for CO oxidation activity. In 1993, Oh and Sinkevitch [26] found that alumina-supported Ru and Rh had higher selectivity and activity than Pt and Pd. Both Ru/Al<sub>2</sub>O<sub>3</sub> and Rh/Al<sub>2</sub>O<sub>3</sub> can achieve nearly complete CO conversion at a temperature near 100°C. Recent work by Rosso et al. [27] showed the activity and selectivity comparison among different noble metals (Pd, Ru, Pt) impregnated on varying types of zeolites (3A, 4A, 5A). Among the noble metals, the Pt catalysts showed the highest CO conversion and selectivity. For Pt catalysts, Pt supported on 3A-zeolite showed the highest selectivity for CO oxidation and minimum side reaction, such as H<sub>2</sub> oxidation and reverse-water-gas shift reaction.

The effect of water vapor reported from many labs is still inconclusive. It depends on not only the type of the catalyst (active metal and support material) but also the reaction temperatures and partial pressure of water vapor. The study reported by Korotkikh and Farrauto [19] showed a decrease in CO oxidation activity with 3% water addition for Pt/alumina catalyst. In contrast, studies by Nibbelke et al. [28], Manasilp and Gulari [18], Kahlich et al. [17], and Avgouropoulos et al. [29] showed that the presence of steam enhanced the catalyst activity, especially at low steam partial pressures. The effect of water vapor on Au-based catalysts is more conclusive. As reported in many studies [24], [30-32], water vapor enhances the CO<sub>2</sub> production rate on Au.

Lately, membrane has been integrated to enhance the selectivity of CO oxidation. Different types of supported metals were loaded on the membrane surface as an oxidation catalyst such as PtY [33-35], Pt, Ru, Ni and Co on  $\gamma$ -Al<sub>2</sub>O<sub>3</sub> [36], Rh/ $\gamma$ -Al<sub>2</sub>O<sub>3</sub> [34]. It was found that in all reported cases above that catalytic membrane improved the selectivity towards CO<sub>2</sub> compared to the same catalyst without membrane at similar conditions.

In this study, we will simulate the result when treating the product gas from LTS in a selective oxidation reactor at  $100^{\circ}$ C, the temperature compatible with PEM fuel cell operation. The activity and selectivity of the selective oxidation catalyst can be reasonably assumed from available literatures. For roughly calculation, important assumption is that selectivity and activity are independent of feed composition. One hundred moles per second of total gas feed rate is used as a basis of calculation. The amount of catalyst required to reduce CO down to a few ppm and the percentage of hydrogen loss during the selective CO oxidation process over  $Pt/\gamma$ - $Al_2O_3$  catalyst when varying the temperature in reformer are shown in Fig 7.

**Table 2:** The CO oxidation rate and CO<sub>2</sub> selectivity of selected selective oxidation catalysts.

U	•			
	Catalyst	CO oxidation rate	CO <sub>2</sub> selectivity	Ref.
		$(\mu mol/g_{cat}/s)$		
	5%Pt/γ-Al <sub>2</sub> O <sub>3</sub>	1.55 @100°C	34%	[37]
	5%Pt-Fe/γ-Al <sub>2</sub> O <sub>3</sub>	4.3 @90°C	50%	[38]
	0.4% Au/γ-Al <sub>2</sub> O <sub>3</sub>	25 @100°C	50%	[23]
	$3\%$ Au/ $\alpha$ -Fe <sub>2</sub> O <sub>3</sub>	14.13 @100°C	45%	[29]

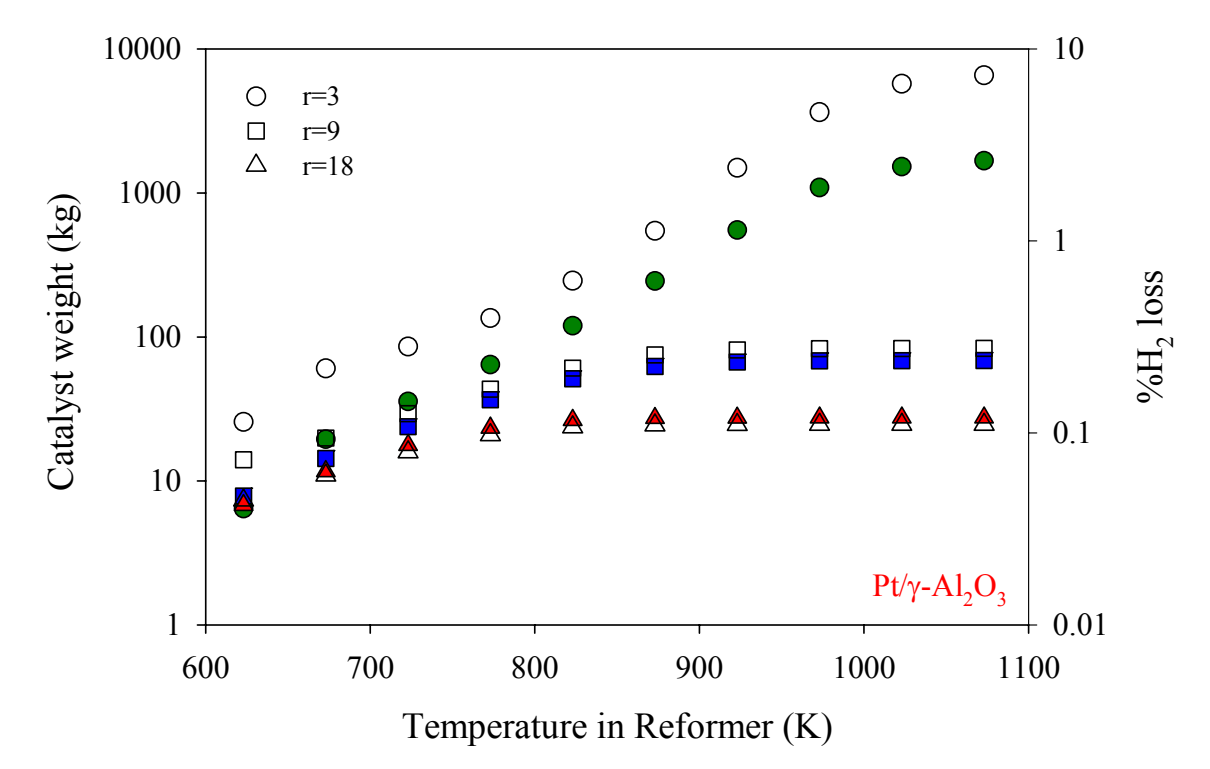


**Figure 7:** Amount of  $Pt/\gamma$ -Al<sub>2</sub>O<sub>3</sub> catalyst required to remove CO down to a few ppm (filled symbols) and the percentage of hydrogen loss during the selective oxidation process at  $100^{\circ}$ C (open symbols) as a function of temperature in reformer.

From Fig.7, it is clearly seen that variation of the amount of catalyst required to reduce CO down to a few ppm with temperature in reformer is similar to that of the percentage of hydrogen loss during the selective oxidation process. When increasing steam/ethanol ratio, less amount of catalyst is required and smaller amount of hydrogen (%) is consumed. Therefore, during the economic evaluation, not only the size of reformer and selective oxidation reactor should be traded off but also the percentage power loss from the amount of hydrogen consumed should be considered. The size of the selective oxidation reactor depends strongly on the activity of the selective oxidation catalyst. For example, at r=3, the amount of catalysts when using different types of catalysts as shown in Table 2 are plotted and shown in Fig. 8. With high amount of CO,

larger amount of catalyst is required at high steam reformer temperature when using low activity catalyst, i.e.  $Pt/\gamma$ -Al<sub>2</sub>O<sub>3</sub> catalyst in this study. Price and lifetime of catalyst will play an important role in scaling-up this process.

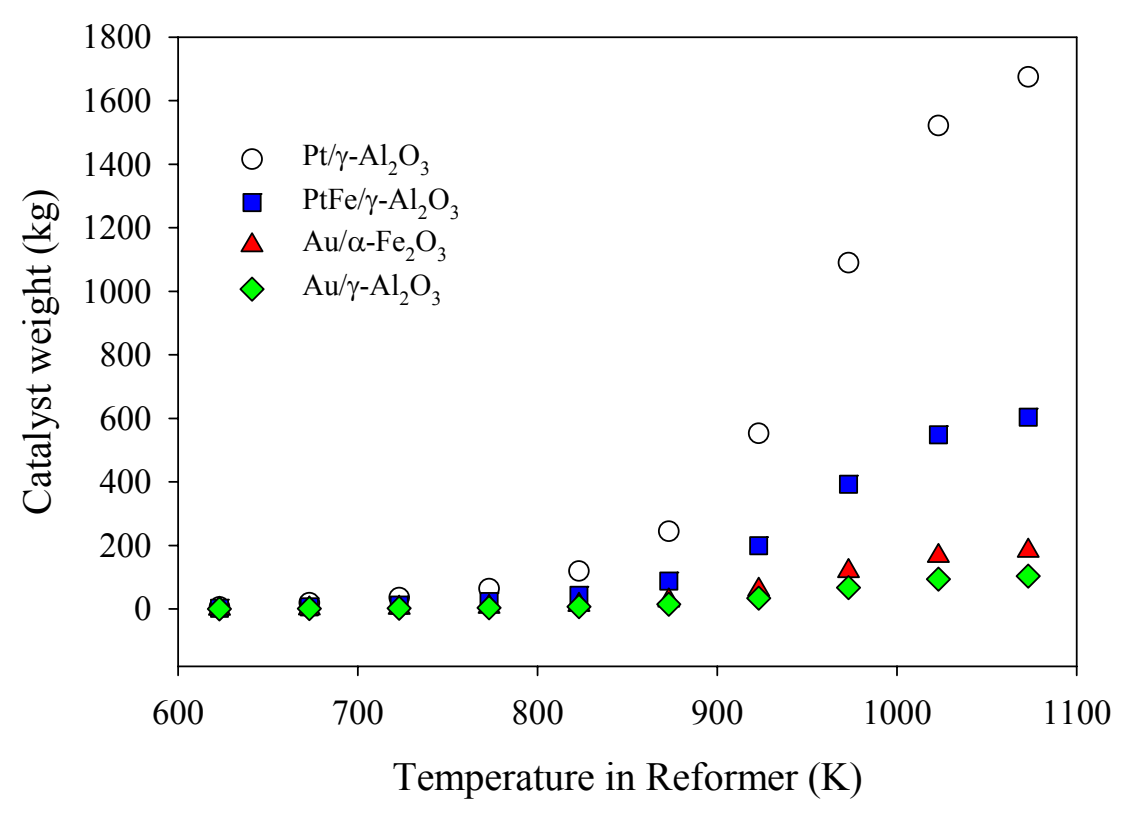


**Figure 8:** The variation of catalyst weight in the selective oxidation reactor required to remove CO down to a few ppm with temperature in reformer at steam/ethanol ratio equal to 3 when using 5%Pt/ $\gamma$ -Al<sub>2</sub>O<sub>3</sub>, 5%Pt-Fe/ $\gamma$ -Al<sub>2</sub>O<sub>3</sub>, 0.4% Au/ $\gamma$ -Al<sub>2</sub>O<sub>3</sub> or 3%Au/ $\alpha$ -Fe<sub>2</sub>O<sub>3</sub> catalyst. The selective oxidation temperature is indicated for each catalyst in Table 2.

# 4. Conclusions

From the thermodynamic analysis, in order to produce hydrogen stream suitable for fuel cell application, moderate reformer temperature and high steam/ethanol ratio are preferable. To be used with solid oxide fuel cell (~1% CO tolerance) without further treatment, reformer temperature has to be lower than 700 K but will result in low hydrogen yield even at high steam/ethanol ratio. The product gas quality can be improved by passing through a low-temperature shift reactor. The thermodynamic analysis shows that by passing through an LTS at 200°C, the quality of product gas is significantly improved and a wide range of reformer operating conditions can be used to produce hydrogen stream for solid oxide fuel cell. However, for PEM fuel cell, the only possible operating condition is that the reformer temperatures to be lower than 623 K and steam/ethanol ratio higher or equal to 18. This condition will result in low hydrogen yield,

which is not economically attractive. Therefore, to decrease the CO content while maintaining high hydrogen yield, another treatment such as selective oxidation reactor should be included. The calculation shows that at higher steam/ethanol ratio in reformer, even though it results in larger reformer, smaller selective oxidation reactor is required. Therefore, sizes of reformer and selective oxidation reactor, heat load and catalyst price for both reactors have to be included during the process design

# Approach to equilibrium for ethanol steam reforming over cobalt, rhodium and nickel based catalysts

## 1. Introduction

Ethanol produced from the fermentation of biomass is an environmentally friendly source for hydrogen production. Steam reforming process is incorporated to convert ethanol to hydrogen and other carbon-containing products. Although, in general, the main reaction of ethanol steam reforming can be written as:

$$C_2H_5OH + 3H_2O \rightarrow 6H_2 + 2CO_2$$
 (1)

There are actually many reactions occurring in the reformer including ethanol decomposition, water-gas-shift and steam reforming of methane. Hence, excluding CO<sub>2</sub>, other carbon containing species such as CO and CH<sub>4</sub> are also generated. Although, the composition at equilibrium can be predicted, the composition of product gas in actual operation depends on the activity and selectivity of the reformer catalyst towards these reactions. In addition, the extent of equilibrium approach and how the equilibrium is approached will also be important factors.

In this study, the composition at equilibrium was determined using Lagrange's undetermined multipliers. If following the method proposed by Mas et al. [1], the influence of water-gas shift and methane steam reforming reaction coordinate can be seen. Except the two schemes proposed by Mas et al. [1] for ethanol conversion, one more scheme was proposed in this study to better explain the results. The equilibrium results were compared with experimental results on Co, Ni and Rh –based catalysts, highly available metals being studied. From the comparison, the influence of catalytic activity on the product gas composition can be evaluated.

# 2. Experimental

# 2.1 Equilibrium calculation

At specified temperature and pressure, the equilibrium amount of ethanol, hydrogen, carbon dioxide, carbon monoxide, methane and water at the condition of interest can be determined based on the method of Lagrange's undetermined multipliers [14] as explained in the previous chapter. In addition, if we follow the method explained by Mas et.al. [1], which to propose sets of independent reactions, we can see the effect of each reaction coordinate on the equilibrium composition. After that the number of moles of all components can be written as functions of water-gas shift conversion  $(X_{WGS})$  and methane steam reforming conversion  $(X_{SRM})$  as follows.

	Scheme A	Scheme B	Scheme C
Hydrogen	$1+X_{WGS}+3X_{SRM}$	$2+X_{WGS}+3X_{SRM}$	$4+X_{WGS}+3X_{SRM}$

Carbon dioxide	$X_{ m WGS}$	$1+X_{WGS}$	$X_{ m WGS}$
Carbon monoxide	$1-X_{WGS}+X_{SRM}$	$-X_{WGS} + X_{SRM}$	$2-X_{WGS} + X_{SRM}$
Methane	$1-X_{SRM}$	$1-X_{SRM}$	- $X_{SRM}$
Water	r- X <sub>WGS</sub> - X <sub>SRM</sub>	r-1- X <sub>WGS</sub> - X <sub>SRM</sub>	r-1- X <sub>WGS</sub> - X <sub>SRM</sub>

 $X_{WGS}$  and  $X_{SRM}$  stand for equilibrium conversions of water-gas shift and methane steam reforming reactions, respectively.

The reactions are assumed to occur sequentially from ethanol conversion to WGS and/ or SRM. Initially when no WGS or SRM has not progressed ( $X_{WGS}=0$ ,  $X_{SRM}=0$ ), the composition of the dry-gas product would be as what is shown in Table 1.

**Table 1:** The initial product composition in dry gas before water-gas shift and methane steam reforming reactions have progresses for different schemes.

	Scheme A	Scheme B	Scheme C
Hydrogen	33.3%	50%	67.7%
Carbon dioxide	0.0%	25%	0%
Carbon monoxide	33.3%	0%	33.3%
Methane	33.3%	25%	0

The results from this part can be used to investigate the effect of catalytic activity on the product composition when actual operation is not at equilibrium. With an assumption that ethanol conversion occurs first followed by two competitive reactions (WGS and SRM), product composition obtained from the real steam reforming process has to be between the initial composition in the table above and the equilibrium composition at the condition of interest.

# 2.2 Calculation

In order to convert all experimental results from the literature in to the same basis, some of them are recalculated into %dry gas composition and mole of hydrogen per mole of converted ethanol according to the definition provided in that corresponding work.

# 3. Results & Discussion

# 3.1 Equilibrium composition

When varying reformer temperatures from 523 K to 1173 K and steam/ethanol ratios from 3 to 9 and 18, compositions of dry gas at equilibrium are shown in Fig. 1. The equilibrium conversion for other conditions reported in the literature will be calculated by following the same method. Comparison between equilibrium values and experimental data will be made to justify the reaction scheme proposed by Mas et al. [1] and the one

proposed in this work.

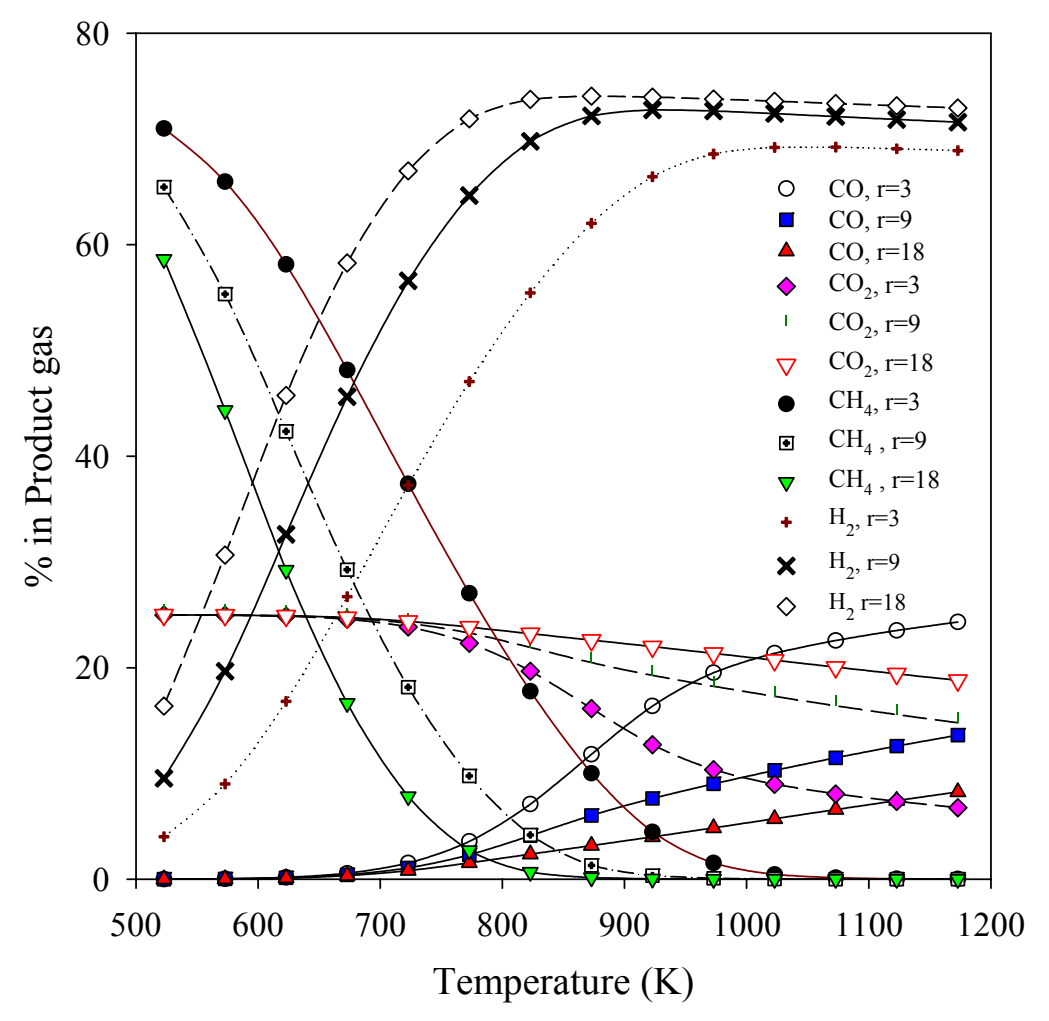


**Figure 1.** The equilibrium composition in dry gas product when varying steam/ethanol ratios and temperatures.

# 3.2 Comparison with experimental result

# 3.2.1 Cobalt-based catalysts

The use of cobalt-based catalysts for ethanol steam reforming has been studied by many research groups. Haga et al. [7] is one of the first researchers focusing on the effect of supports on the catalytic properties of cobalt catalysts. Product composition obtained when using cobalt catalysts with different supports at 673 K and steam/ethanol ratio of 4.23 is shown in Table 2 in comparison with the equilibrium composition at the same reaction condition. All catalysts used provided higher amount of hydrogen and carbon monoxide and lower amount of methane in product gas compared to the values at equilibrium. This result could not be explained by two reaction schemes proposed by Mas [1] but consistent with scheme C proposed in this study. In addition, the compositions of all components in the product fall between the initial value for Scheme C (Table 1) and the equilibrium values. These indicate that the reaction on cobalt-based catalysts

approached equilibrium from initially high hydrogen, high carbon monoxide and low methane side, which is the ethanol steam reforming via scheme C, not the decomposition path. Number of moles of hydrogen per mole of converted ethanol is ranged between 2.8 - 4.1, when, at equilibrium, it is only 1.0. It suggests that ethanol was converted mostly via scheme C ( $C_2H_5OH + H_2O= 2CO+4H_2$ ) with methane and carbon dioxide generation afterward via CO methanation and WGS. It was confirmed by the experimental data reported by Batista et al. [9] at the same temperature but lower steam/ethanol ratio (#8,9) that at 673 K, ethanol was converted via steam reforming to form two moles of CO and four moles of hydrogen. In contrast, it is surprising that at higher temperature (873 - 973)K) and steam/ethanol ratio (r=9.7), as reported by Benito et al. [39], the ethanol conversion mechanism seems to change to decomposition, observed from the amount of CH<sub>4</sub> which is higher than equilibrium value and falls between the equilibrium value and the initial value for scheme A. This suggests that reaction temperature has more effect on reaction mechanism than the steam/ ethanol ratio has. In addition, according to the number of moles of hydrogen generated per mole of converted ethanol, the steam reforming reaction should be operated far from equilibrium if operating at low temperatures (<673 K) and close to equilibrium if operating at high temperatures (>823 K) to have the highest hydrogen produced per mole ethanol.

**Table 2:** Dry gas composition of main products and number of moles hydrogen per mole converted ethanol for selected cobalt-based catalysts

Set#	Catalyst	Product composition (%)				Mole H <sub>2</sub> /mole
		$H_2$	$CO_2$	СО	CH <sub>4</sub>	converted ethanol
1	Equilibrium at 673 K (r=4.2)	32	24.6	0.5	42.8	0.9
2	7.4%Co/Al <sub>2</sub> O <sub>3</sub> <sup>a</sup>	67	19	7.9	6.0	4.1
3	7.4%Co/ZrO <sub>2</sub> <sup>a</sup>	65	23	3.1	8.9	3.7
4	7.4%Co/MgO <sup>a</sup>	65	23	2.5	9.2	3.7
5	7.4%Co/SiO <sub>2</sub> <sup>a</sup>	63	24	2.0	11.0	3.4
6	7.4%Co/C <sup>a</sup>	58	23	2.4	16.0	2.8
7	Equilibrium at 673 K (r=3)	27	25	0.6	48	0.7
8	8%CO/SiO <sub>2</sub> <sup>b</sup>	67	11	10	12	4.1
9	18%CO/SiO <sub>2</sub> <sup>b</sup>	67	24	2	7	4.1
10	Equilibrium at 873 K (r=9.7)	72.5	20.8	5.7	1.1	5.3
11	Co/ZrO <sub>2</sub> <sup>c</sup>	70	19	8	3.0	4.7
12	Equilibrium at 973 K (r=9.7)	73	18.7	8.5	0.07	5.4
13	Co/ZrO <sub>2</sub> <sup>c</sup>	67	17.5	11	5	4.0

<sup>&</sup>lt;sup>a</sup>Data from Haga et al.[7] at 673 K and r= 4.2

<sup>&</sup>lt;sup>b</sup> Data from Batista et al.[9] at 673 K and r= 3

<sup>&</sup>lt;sup>c</sup>Data from Benito et al. [39] at T=973 K and r=9.7

# 3.2.2 Rhodium-based catalysts

**Table 3:** Dry gas composition of main products and number of moles hydrogen per mole converted ethanol for selected rhodium-based catalysts

Set#	Catalyst	Product composition (%)			Mole H <sub>2</sub> /mole	
		$H_2$	$CO_2$	СО	$\mathrm{CH_4}$	converted ethanol
1	Equilibrium at 973 K (r=3)	68.6	10.4	19.5	1.5	4.4
2	$1\%$ Rh/ $\gamma$ -Al $_2$ O $_3$ $^a$	72	21	7	0	5.1
3	Equilibrium at 973 K (r=4)	70.0	12.6	16.5	0.8	4.7
4	$0.3\%$ Rh/ $\gamma$ -Al $_2$ O $_3$ $^b$	59.6	14.6	11.7	14.0	3.0
5	$0.9\%$ Rh/ $\gamma$ -Al $_2$ O $_3$ $^b$	60.7	16.5	10.3	12.2	3.1
6	Equilibrium at 923 K (r=5)	70.3	15.9	12.1	1.6	4.8
7	$1\%$ Rh/ $\gamma$ -Al <sub>2</sub> O <sub>3</sub> <sup>c</sup>	70.6	13.3	16.2	0	4.8
8	Equilibrium at 923 K (r=8.4)	72.6	18.9	8.1	0.4	5.3
9	5%Rh/γ-Al <sub>2</sub> O <sub>3</sub> d	73.3	20.0	6.4	0.3	5.5
10	5%Rh/γ-Al <sub>2</sub> O <sub>3</sub> <sup>e</sup>	69.2	17.2	9.6	3.9	4.5
11	3%Rh/MgO <sup>f</sup>	73.4	16.5	7.2	2.9	5.5

<sup>&</sup>lt;sup>a</sup> Data from Aupretre et al. [5] at 973 K, r=3

The activity of Rhodium-based catalysts for ethanol steam reforming has been studied extensively by Aupretre et al. [5, 40], Montini et al. [41], Cavallaro et al. [12] Freni [42] and Frusteri et al. [43] since they are highly active for this reaction. All available data are conducted at high temperatures (923 -973 K) because lots of other byproducts such as CH<sub>2</sub>CH<sub>2</sub> can be generated at temperature lower than 823 K. Compositions of main dry gas products calculated from their results are shown in Table 3 in comparison with the values from equilibrium calculation. The comparison shows that at this high temperature, the amount of hydrogen in dry gas is close to the equilibrium value in almost all cases. In addition, within experimental error all results go in the same direction that the amount of CO<sub>2</sub> and CH<sub>4</sub> from experiment is higher than equilibrium values (except set#1,7) whereas the amount of CO from experiment is lower than the equilibrium one. Data in set#7 are quite close to the equilibrium values, thus, it is difficult to justify about its ethanol conversion path. From these observations, it is suggested that the ethanol conversion when using Rh/γ-Al<sub>2</sub>O<sub>3</sub> catalyst at these high temperatures seems to be via scheme B, steam reforming to methane, carbon dioxide and hydrogen and it is independent of the steam/ethanol ratio. Steam/ethanol ratio seems to have no effect on the

<sup>&</sup>lt;sup>b</sup> Data from Aupretre et al. [40] at 973 K, r=4

<sup>&</sup>lt;sup>c</sup> Data from Montini et al. [41] at 923 K, r=5

<sup>&</sup>lt;sup>d</sup> Data from Cavallaro et al. [12] at 923 K, r=8.4

e Data from Freni [42] at 923 K, r=8.4

f Data from Frusteri et al. [43] at 923 K, r=8.4

ethanol conversion path. In addition, for this type of catalysts and at high temperature, longer contact time is preferable for higher hydrogen yield.

# 3.2.3 Nickel-based catalysts

Nickel-based catalyst has been studied extensively by Comas et al. [4], Sun et al. [44], Barroso et al. [45], Auprete et al. [5] and Benito et al. [39]. From the data reported by Comas et al. [4] and Sun et al. [44] at low temperature and low steam/ethanol ratio (set# 2,3), the amount of hydrogen and carbon monoxide in dry gas product are higher whereas that of carbon dioxide and methane are lower than the equilibrium values at similar condition. In addition, these values are between the initial values for Scheme C and the equilibrium values. When increasing reforming temperature to 673 K and 773 K at the same steam/ethanol ratio, the same behavior is observed. The NiZnAl catalysts (NZA) with varying amount of Ni was studied by Barroso et al. [45] at 873 K of reformer temperature and steam/ethanol ratio equal to 3.6. At this condition, the experimental values are quite close to the equilibrium ones. However, similar observations as for the case of Ni/Al<sub>2</sub>O<sub>3</sub> and Ni/Y<sub>2</sub>O<sub>3</sub> at lower temperature can be made. Unfortunately, for Ni/Y<sub>2</sub>O<sub>3</sub> catalyst, when increasing reformer temperature to 873 K, it behaves differently from what it does at lower temperature. The experimental values for this data set (#14) are between the initial values for Scheme B and the equilibrium values. Not only in Ni/Y<sub>2</sub>O<sub>3</sub> catalyst, the change in ethanol conversion path from scheme C to scheme B was also observed in Ni/Al<sub>2</sub>O<sub>3</sub> catalyst. At 973 K and similar steam/ethanol ratio for the Ni/Al<sub>2</sub>O<sub>3</sub> catalyst studied by Auprete et al. [5], the experimental values fall between the equilibrium values and the initial values in Scheme B instead of Scheme C as it does at low temperatures. At this high temperature (973 K) and higher steam/ethanol ratio, experimental results on Ni/ZrO<sub>2</sub> reported by Benito et al. [39] showed that this catalyst gave the composition of dry gas close to equilibrium. Thus, it is difficult to justify this catalyst at this condition. Therefore, at this point, it can be concluded that over nickel-based catalysts appeared in this work, their ethanol conversion path seems to change from Scheme C to Scheme B when increasing reformer temperature at steam/ethanol ratio approximately equal to 3. Following this conclusion, short contact time is preferable at low reformer temperature but longer contact time is needed at higher reformer temperature (>873K). Due to the lack of reported data, the behavior of nickel catalyst at higher steam/ethanol ratios cannot be justified.

**Table 4:** Dry gas composition of main products and moles of hydrogen per mole of converted ethanol for selected nickel-based catalysts

Set#	Catalyst	Product composition (%)				Mole H <sub>2</sub> /mole
		$H_2$	$CO_2$	CO	CH <sub>4</sub>	converted ethano
1	Equilibrium at 573 K (r=3.3)	9.7	25	0.04	65.3	0.2
2	35%Ni/Al <sub>2</sub> O <sub>3</sub> <sup>a</sup>	38.3	4.4	28.7	28.7	1.2
3	$Ni/Y_2O_3^b$	38	18	9	35	1.2
4	Equilibrium at 673 K (r=3.3)	28.1	24.6	0.5	46.7	0.8
5	35%Ni/Al <sub>2</sub> O <sub>3</sub> <sup>a</sup>	46.7	22.7	1.3	28.4	1.8
6	$Ni/Y_2O_3^b$	43	19	0	38	1.5
7	Equilibrium at 773 K (r=3.3)	48.7	22.4	3.5	25.4	1.9
8	35%Ni/Al <sub>2</sub> O <sub>3</sub> <sup>a</sup>	58.2	20.2	7.5	14.1	2.8
9	$Ni/Y_2O_3^b$	49	20	1	30	1.9
10	Equilibrium at 873 K (r=3.6)	64.3	16.9	10.8	8	3.6
11	NZA8 <sup>c</sup>	67.8	14.6	10.3	7.4	4.2
12	NZA18 <sup>c</sup>	72.2	10.3	16.1	1.4	5.2
13	NZA25 <sup>c</sup>	71.4	11.6	16.1	0.9	5.0
14	$Ni/Y_2O_3^b$	57	21	5	17	2.7
15	Equilibrium at 973 K (r=3)	68.6	10.4	19.5	1.5	4.4
16	$9.7\%$ Ni/ $\gamma$ -Al <sub>2</sub> O <sub>3</sub> <sup>d</sup>	70.5	18	11	0.5	4.8
17	Equilibrium at 973 K (r=9.7)	73	18.7	8.5	0.07	5.4
18	Ni/ZrO <sub>2</sub> <sup>e</sup>	67	18	10	4	4.2

<sup>&</sup>lt;sup>a</sup> Data from Comas et al. [4] at 573 K, r=3.3

# 3.3 Proposed model

The ethanol conversion path for each scheme was proposed as shown in Fig. 2. Firstly, for all schemes, both ethanol and water molecule are adsorbed on the metal surface before the ethanol molecule is decomposed to CH<sub>4</sub>, H<sub>2</sub> and CO. In scheme A, the decomposition products do not have an opportunity to react with adsorbed water because the desorption rate is much faster than rate of the reaction. In contrast, for scheme B and C, the rate of reacting with adsorbed water is faster than the desorption rate of the product. Therefore, adsorbed water can react with CO to form CO<sub>2</sub> and H<sub>2</sub> for scheme B or with CH<sub>4</sub> to form CO and 2 moles of H<sub>2</sub> for scheme C, depending on the catalytic activity toward water-gas-shift or methane steam reforming reaction. The adsorption strength of each decomposition product on the metal surface also affects the ethanol conversion path. Species that is strongly adsorbed on the surface will have more chance to react with adsorbed water molecule nearby. As in the case of cobalt catalyst at low temperature, it is highly possible that the adsorption strength of methane is larger than

<sup>&</sup>lt;sup>b</sup>Data from Sun et al. [44] at r=3

<sup>&</sup>lt;sup>c</sup>Data from Barroso et al. 2006 [45] at 873 K, r=3.6

<sup>&</sup>lt;sup>d</sup>Data from Auprete et al. [5] at 973 K, r=3

<sup>&</sup>lt;sup>e</sup>Data from Benito et al. [39] at T=973 K and r=9.7

other species on the cobalt catalyst. The change in ethanol conversion path for cobalt-based catalysts from Scheme C to scheme A can be explained by the increase in the desorption rate of all decomposition products at higher temperature. For nickel-based catalysts, the adsorption strength of CH<sub>4</sub> that might be weaker at higher temperature compared to that of CO may cause the change in ethanol conversion path from scheme C to scheme B when temperature was increased.

## 4. Conclusion

From all comparisons presented above, although available data cannot cover a wide range of reformer temperatures and steam/ethanol ratios, it is obviously seen that temperature has significant effect on that the way to approach equilibrium and seems to vary with type of catalyst. In contrast, the steam/ethanol ratio has no observed effect on ethanol conversion path but will affect the equilibrium composition by accelerating or inhibiting the water-gas-shift or methane steam reforming reaction. The results also showed that the two schemes proposed by Mas et al. [1] cannot explain the experimental values when using cobalt and nickel-based catalysts. After looking deeper into Scheme B and C, Scheme B is, in fact, the combination of ethanol decomposition and water-gas-shift reaction whereas Scheme C is the combination of ethanol decomposition and methane steam reforming reaction when these two reactions occur simultaneously. Therefore, it is suggested that the difference in ethanol conversion path seems to depend on the catalytic activity of the catalyst toward water-gas-shift and methane steam reforming reactions. Except when operating at equilibrium, nature of catalyst and reaction

temperature, thus, play an important role on the reaction scheme. From this information, appropriate operating condition can be chosen to have the desired product gas composition. At a fixed temperature and type of catalyst, the reaction residence time or space velocity can be control to improve the product gas quality.

## References

- 1. Mas, V., et al., *Thermodynamic analysis of ethanol/water system with the stoichiometric method.* International Journal of Hydrogen Energy, 2006. **31**(1): p. 21-28.
- 2. Liguras, D.K., D.I. Kondarides, and X.E. Verykios., *Production of hydrogen for fuel cells by steam reforming of ethanol over supported noble metal catalysts*. Applied Catalysis B: Environmental, 2003. **43**: p. 345-354.
- 3. Goula, M.A., S.K. Kontou, and P.E. Tsiakaras, *Hydrogen production by ethanol steam reforming over a commercial Pd/γ-Al<sub>2</sub>O<sub>3</sub> catalyst.* Applied Catalysis B: Environmental, 2004. **49**(2): p. 135-144.
- 4. Comas, J., et al., *Bio-ethanol steam reforming on Ni/Al<sub>2</sub>O<sub>3</sub> catalyst*. Chemical Engineering Journal, 2004. **98**(1-2): p. 61-68.
- 5. Aupretre, F., C. Descorme, and D. Duprez, *Bio-ethanol catalytic steam reforming over supported metal catalysts*. Catalysis Communications, 2002. **3**(6): p. 263-267.
- 6. Batista, M.S., et al., Characterization of the activity and stability of supported cobalt catalysts for the steam reforming of ethanol. Journal of Power Sources, 2003. **124**(1): p. 99-103.
- 7. Haga, F., et al., *Catalytic properties of supported cobalt catalysts for steam reforming of ethanol.* Catalysis Letters, 1997. **48**: p. 223-227.
- 8. Anderson, J.R., Structure of Metallic Catalyst. 1975, New York: Academic Press.
- 9. Batista, M.S., et al., *High efficiency steam reforming of ethanol by cobalt-based catalysts*. Journal of Power Sources, 2004. **134**: p. 27-32.
- 10. Kaddouri, A. and C. Mazzocchia, A study of the influence of the synthesis conditions upon the catalytic properties of Co/SiO<sub>2</sub> or Co/Al<sub>2</sub>O<sub>3</sub> catalysts used for ethanol steam reforming. Catalysis Communications, 2004. **5**(6): p. 339-345.
- 11. Laosiripojana, N. and S. Assabumrungrat, Catalytic steam reforming of ethanol over high surface area CeO<sub>2</sub>: The role of CeO<sub>2</sub> as an internal pre-reforming catalyst. Applied Catalysis B: Environmental, 2006. **66**(1-2): p. 29-39.
- 12. Cavallaro, S., et al., *Performance of Rh/Al<sub>2</sub>O<sub>3</sub> catalyst in the steam reforming of ethanol: H<sub>2</sub> production for MCFC.* Applied Catalysis A: General, 2003. **249**(1): p. 119-128.
- 13. Klouz, V., et al., *Ethanol reforming for hydrogen production in a hybrid electric vehicle: process optimisation.* Journal of Power Sources, 2002. **105**(1): p. 26-34.
- 14. J.M. Smith, H.C.V. Ness, and M.M. Abbott, *Introduction to Chemical Engineering Thermodynamics*. 7th ed. 2005, Singapore: McGraw Hill. 817.
- 15. Brown, M. and A. Green, *US Patent 3,088,919*.
- 16. Igarashi, H., et al., Removal of Carbon Monoxide from Hydrogen-Rich Fuels by Selective Oxidation over Platinum Catalyst Supported on Zeolite. Appl. Catal. A: Gen, 1997. **159**: p. 159.
- 17. Kahlich, M.J., H.A. Gasteiger, and R.J. Behm, *Kinetics of the Selective CO Oxidation in H*<sub>2</sub>-*Rich Gas on Pt/Al*<sub>2</sub>O<sub>3</sub>. J. Catal., 1997. **171**: p. 93.
- 18. Manasilp, A. and E. Gulari, *Selective CO oxidation over Pt/alumina catalysts for fuel cell applications*. Applied Catalysis B: Environmental, 2002. **37**(1): p. 17-25.
- 19. Korotkikh, O. and R. Farrauto, *Selective Catalytic Oxidation of CO in H*<sub>2</sub>: Fuel Cell Applications. Catalysis Today, 2000. **62**: p. 249-254.
- 20. Watanabe, M., et al., *Hydrogen purification for fuel cells: selective oxidation of carbon monoxide on Pt-Fe/zeolite catalysts*. Applied Catalysis B: Environmental, 2003. **46**(3): p. 595-600.
- 21. Grunwaldt, J.-D., et al., Comparative Study of Au/TiO<sub>2</sub> and Au/ZrO<sub>2</sub> Catalysts for

- Low-Temperature CO Oxidation. J. Catal., 1999. 186: p. 458.
- 22. Kahlich, M.J., H.A. Gasteiger, and R.J. Behm, *Kinetics of the Selective Low-Temperature Oxidation of CO in H*<sub>2</sub>-*Rich Gas over Au/α-Fe*<sub>2</sub>*O*<sub>3</sub>. J. Catal., 1999. **182**: p. 430.
- 23. Bethke, G.K. and H.H. Kung, *Selective CO Oxidation in a Hydrogen-Rich Stream over Au/γ-Al<sub>2</sub>O<sub>3</sub> Catalysts*. Appl. Catal. A: Gen, 2000. **194**: p. 43.
- 24. Grisel, R.J.H. and B.E. Nieuwenhuys, *Selective Oxidation of CO over Supported Au Catalysts*. J. Catal., 2001. **199**: p. 48.
- 25. Avgouropoulos, G., et al., *A comparative study of ceria-supported gold and copper oxide catalysts for preferential CO oxidation reaction.* Chemical Engineering Journal, 2006. **124**(1-3): p. 41-45.
- 26. Oh, S.H. and R.M. Sinkevitch, *Carbon Monoxide Removal from Hydrogen-Rich Fuel Cell Feedstreams by Selective Catalytic Oxidation*. J. Catal., 1993. **142**: p. 254.
- 27. Rosso, I., et al., *Development of A zeolites-supported noble-metal catalysts for CO preferential oxidation: H*<sub>2</sub> gas purification for fuel cell. Applied Catalysis B: Environmental, 2004. **48**(3): p. 195-203.
- 28. Nibbelke, R.H., et al., *Kinetic Study of the CO Oxidation over Pt/\gamma-Al<sub>2</sub>O<sub>3</sub> and Pt/Rh/CeO<sub>2</sub>/\gamma-Al<sub>2</sub>O<sub>3</sub> in the Presence of H<sub>2</sub>O and CO<sub>2</sub>. J. Catal., 1997. 171: p. 358.*
- 29. Avgouropoulos, G., et al., A Comparative Study of Pt/γ-Al<sub>2</sub>O<sub>3</sub>, Au/α-Fe<sub>2</sub>O<sub>3</sub> and CuO-CeO<sub>2</sub> Catalysts for the Selective Oxidation of Carbon Monoxide in Excess Hydrogen. Catal. Today, 2002. **75**: p. 257.
- 30. Bulushev, D.A., et al., *Structured Au/FeO<sub>x</sub>/C Catalysts for Low-Temperature CO Oxidation*. J. Catal., 2002. **210**: p. 149.
- 31. Haruta, M., et al., Low-temperature catalytic combustion of methanol and its decomposed derivatives over supported gold catalysts. Catal. Today, 1996. **29**: p. 443.
- 32. Park, E.D. and J.S. Lee, *Effects of Pretreatment Conditions on CO Oxidation over Supported Au Catalysts*. J. Catal., 1999. **186**: p. 1.
- 33. Hasegawa, Y., K. Kusakabe, and S. Morooka, *Selective oxidation of carbon monoxide in hydrogen-rich mixtures by permeation through a platinum-loaded Y-type zeolite membrane*. Journal of Membrane Science, 2001. **190**(1): p. 1-8.
- 34. Sotowa, K.-I., et al., Enhancement of CO oxidation by use of  $H_2$ -selective membranes impregnated with noble-metal catalysts. International Journal of Hydrogen Energy, 2002. **27**(3): p. 339-346.
- 35. Bernardo, P., et al., Catalytic (Pt-Y) membranes for the purification of  $H_2$ -rich streams. Catalysis Today Catalysis in Membrane Reactors, 2006. **118**(1-2): p. 90-97
- 36. Hasegawa, Y., et al., Oxidation of CO in hydrogen-rich gas using a novel membrane combined with a microporous SiO<sub>2</sub> layer and a metal-loaded γ-Al<sub>2</sub>O<sub>3</sub> layer. Applied Catalysis A: General, 2002. **225**(1-2): p. 109-115.
- 37. Sirijaruphan, A., J. Goodwin, James G., and R.W. Rice, *Effect of temperature and pressure on the surface kinetic parameters of Pt/γ-Al<sub>2</sub>O<sub>3</sub> during selective CO oxidation*. Journal of Catalysis, 2004. **227**(2): p. 547-551.
- 38. Sirijaruphan, A., J.G. Goodwin, and R.W. Rice, *Effect of Fe promotion on the surface reaction parameters of Pt/\gamma-Al<sub>2</sub>O<sub>3</sub> for the selective oxidation of CO. Journal of Catalysis, 2004. 224(2): p. 304-313.*
- 39. Benito, M., et al., *Bio-ethanol steam reforming: Insights on the mechanism for hydrogen production.* Journal of Power Sources, Selected papers presented at the First Congress of Fuel Cells in Spain (CONAPPICE 2004), 2005. **151**: p. 11-17.

- 40. Aupretre, F., C. Descorme, and D. Duprez, *Hydrogen production for fuel cells from the catalytic ethanol steam reforming*. Topics in Catalysis, 2004. **30/31**: p. 487-491.
- 41. Montini, T., et al., Rh(1%)@  $Ce_xZr_{1-x}O_2$ - $Al_2O_3$  nanocomposites: Active and stable catalysts for ethanol steam reforming. Applied Catalysis B: Environmental, 2007. **71**(3-4): p. 125-134.
- 42. Freni, S., *Rh based catalysts for indirect internal reforming ethanol applications in molten carbonate fuel cells.* Journal of Power Sources, 2001. **94**(1): p. 14-19.
- 43. Frusteri, F., et al.,  $H_2$  production for MC fuel cell by steam reforming of ethanol over MgO supported Pd, Rh, Ni and Co catalysts. Catalysis Communications, 2004. **5**(10): p. 611-615.
- 44. Sun, J., et al., *Hydrogen from steam reforming of ethanol in low and middle temperature range for fuel cell application*. International Journal of Hydrogen Energy Fuel Cells, 2004. **29**(10): p. 1075-1081.
- 45. Barroso, M.N., et al., *Hydrogen production by ethanol reforming over NiZnAl catalysts*. Applied Catalysis A: General, 2006. **304**: p. 116-123.

# Output ที่ได้จากโครงการ

- 1. Sirijaruphan, A., and Praserthdam, P. "Thermodynamic Calculation of the Ethanol Steam Reforming Reaction: Possibility to Produce Low-Carbon Monoxide Hydrogen Stream" The 2<sup>nd</sup> International Conference on Advances in Petrochemicals and Polymers, Bangkok, Thailand. June 2007.
- 2. Sirijaruphan, A., and Praserthdam, P., "The study on the effect of ethanol concentration on Co/SiO<sub>2</sub> catalyst for the steam reforming of ethanol" submitted to the KMUTT research and development journal.

ภาคผนวก

# Thermodynamic Calculation of the Ethanol Steam Reforming Reaction: Possibility to Produce Low-Carbon Monoxide Hydrogen Stream

Amornmart Sirijaruphan \*,1, Piyasan Praserthdam 2

<sup>1</sup>Department of Chemical Engineering, King Mongkut's University of Technology Thonburi, Bangkok, Thailand; <sup>2</sup>Department of Chemical Engineering, Chulalongkorn University, Bangkok, Thailand; \*amornmart.sir@kmutt.ac.th **ABSTRACT** 

This study aimed to determine the equilibrium composition of the ethanol steam reforming reaction and the possibility to produce low-carbon monoxide hydrogen stream. Sets of three independent reactions were individually used to calculate the compositions of the product gases from the ethanol steam reforming reaction when varying steam/ethanol ratios,r, (3, 9, 18) and temperatures (523 K-1173 K). At these high temperatures, the complete conversion of ethanol by i) decomposition or ii) steam reforming can be reasonably assumed. Each set of independent equations consisted of i) ethanol conversion reaction, ii) water-gas-shift reaction, and iii) methane steam reforming. Despite the difference in ethanol conversion paths, the same thermodynamic equilibrium composition was obtained. The results showed that high steam/ethanol ratio was preferable for high hydrogen yield and low carbon monoxide generation. Although high temperature was preferable for high hydrogen yield, high amount of carbon monoxide was also generated at this condition. The results also showed that it was possible to produce low-carbon monoxide hydrogen stream to be used in PEM fuel cell (<100 ppm) after treated in a lowtemperature shift reactor or to be used with solid oxide fuel cell (<5000 ppm) without any treatment when operating at high steam/ethanol ratios (i.e., 18) and temperatures lower than ~650 K. At higher temperatures or lower steam/ethanol ratios, selective CO oxidation reactor was necessary in producing PEMFC hydrogen feed stream. Trading off among reformer size, lowtemperature shift reactor size and adding more reactor was also discussed in this study.

## 1. INTRODUCTION

Main fuels used at present come from crude oil refinery. This energy source is limited and will be extinguish within a few decades. This necessity forces researchers to look for other alternative fuels. Fuel derived from biomass is an environmental friendly alternative. Its high availability makes it more attractive especially in agricultural countries like Thailand. The fermentation process can be incorporated to produce ethanol, which can be steam reformed to hydrogen and then further used in fuel cells. The overall process from biomass production to fuel cell operation has zero net carbon dioxide generation.

Although, in general, the main reaction of ethanol steam reforming can be written as:

$$C_2H_5OH + 3H_2O \rightarrow 6H_2 + 2CO_2$$
 (1)

There are actually many reactions occurring in the reformer including ethanol decomposition, water-gas-shift and steam reforming of methane. The composition of the product gas from reformer, thus, depends on the activity of the catalyst towards these reactions. However, if the reformer is operated at equilibrium, the composition will be the same for all catalysts at a given temperature and feed composition.

In this study, the composition at equilibrium was determined using Lagrange's undetermined multipliers. The results were compared with the method proposed by Mas, et al. [1], which provided the equilibrium conversion of each reaction for each proposed mechanism. From the comparison, the influence of catalytic activity on the product gas composition can be evaluated. In addition, the composition of hydrogen stream after being treated in Low-temperature shift reactor was also investigated for the possibility to be used in fuel cells.

## 2. EXPERIMENTAL

# 2.2 Equilibrium calculation by Minimizing total Gibbs energy approach

At a specified temperature and pressure, the set of {n<sub>i</sub>} which minimizes G<sup>t</sup> can be determined based on the method of Lagrange's undetermined multipliers [2] . For the ethanol steam reforming reaction, the equilibrium amounts of ethanol, hydrogen, carbon dioxide, carbon monoxide methane and water were our interest.

Sets of non-linear equations and explicit equations were then used to determine the equilibrium composition when varying reaction temperatures from 523 K to 1173 K and steam/ethanol ratios (r) from 3 to 9 and 18.

## 2.2 Equilibrium calculation by Equilibrium constant approach

Another approach to determine the equilibrium composition is to follow the method explained by Mas et al. [1]. Since there are only three independent atomic species, set of three independent reactions was used in the calculation. Two different schemes of ethanol conversion were proposed in the work reported by Comas, et al. and Mas, et al. [1, 3]. In the first scheme, ethanol was decomposed to 1 mole each of methane, carbon monoxide and hydrogen (C<sub>2</sub>H<sub>5</sub>OH = CH<sub>4</sub>+CO+H<sub>2</sub>). In the other scheme, ethanol was reformed by one mole of water to form 1 mole of methane, 1 mole of carbon dioxide and 2 moles of hydrogen (C<sub>2</sub>H<sub>5</sub>OH + H<sub>2</sub>O= CH<sub>4</sub>+CO<sub>2</sub>+2H<sub>2</sub>). The other two reactions occurred sequentially during the steam reforming process, which were used in the equilibrium calculation were water-gas shift reaction, WGS (CO +  $H_2O$  =  $CO_2$  +  $H_2$ ) and the steam reforming of methane, SRM ( $CH_4 + H_2O = CO + 3H_2$ ). The equilibrium conversion of ethanol was close to 100% at all temperatures above 500 K [1]. Therefore, total conversion of ethanol was assumed. Assuming ideal gas at this condition, set of non-linear equations can be solved by using Newton method in the Polymath program. The number of moles of all components can be written as functions of WGS conversion (X<sub>WGS</sub>) and SRM conversion (X<sub>SRM</sub>). The equilibrium constant for each reaction at the temperature of interest was inserted into the non-linear equations and set of equations was then solved for X<sub>WGS</sub> and X<sub>SRM</sub>.

## 3. RESULTS & DISCUSSION

## 3.1 Equilibrium composition

After the result was generated, it can be used to confirm the complete conversion of ethanol as previously assumed in section 2.2. It is worth noting that the mole fraction of ethanol in the product is less than  $10^{-11}$  in all cases. Compositions of dry gas products at different temperatures and steam/ethanol ratios are shown in Fig. 1. It is not surprising that both approaches provided the same results. In addition, both schemes in the equilibrium constant approach gave the same equilibrium amounts of products. However, the equilibrium conversions for WGS and SRM are different from one scheme to the other as shown in Fig. 2. As can be clearly seen in Fig 1, high temperatures of up to  $\sim 900$  K are preferable for high hydrogen content. However, at these high temperatures, high amount of carbon monoxide is also produced. Although the amount of hydrogen can be increased and the amount of carbon monoxide can be decreased by increasing the steam/ethanol ratio, the amount of carbon monoxide in product gas is still too high ( $\sim 3.2\%$  at 873 K, r=18). Thus, further treatment is required.

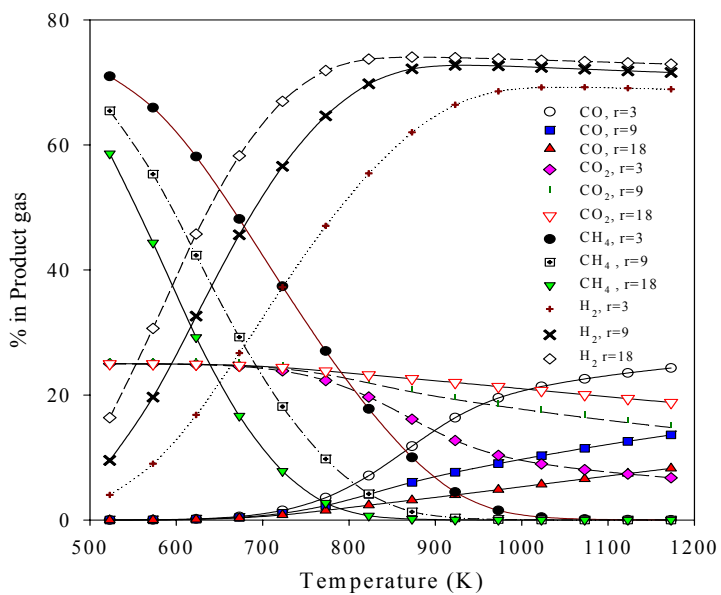


Figure 1: The equilibrium composition in dry gas product when varying steam/ethanol ratios and temperatures

The equilibrium calculation results in terms of  $X_{WGS}$  and  $X_{SRM}$  are shown in Fig. 2. Similar shape of both equilibrium conversions was obtained in both schemes despite their different starting and end points. Since water-gas shift reaction is exothermic, its equilibrium conversions reach a maximum at around 810-830 K before starting to decrease. In both schemes, increasing steam/ethanol ratio resulted in the increase in both water-gas-shift and methane steam reforming conversions. With different ethanol conversion paths,  $X_{WGS}$  and  $X_{SRM}$  were adjusted until reaching

the product composition that provides the lowest Gibbs free energy of the system at that particular temperature. In the real operation, which might be far from equilibrium, one would expect that the composition of the product gas would depend on the activity of the catalyst toward WGS and SRM reactions.

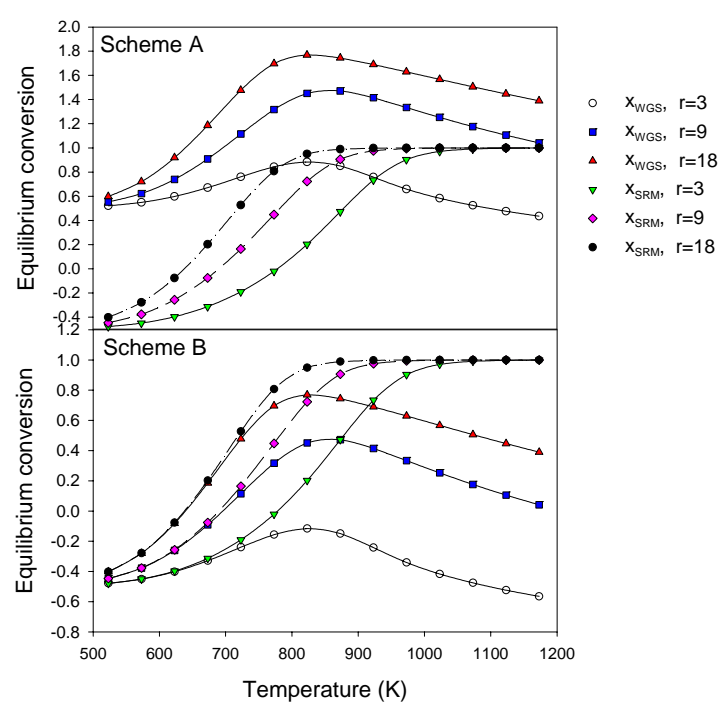


Figure 2: Equilibrium conversions for water-gas-shift reaction and methane steam reforming reaction from the calculation using scheme A and B.

### 3.2 Role of catalysts

During the steam reforming of ethanol, catalyst would play an important role on the rate of approaching equilibrium. If the catalyst is not active for either one of the three reactions (ethanol conversion, WGS or SRM), operating at equilibrium condition is impossible and the product composition will be different from the equilibrium values shown in Fig. 1. For example, if the catalyst is active for only ethanol decomposition and steam reforming of methane, water-gas-shift reaction would be suppressed and carbon dioxide could not be generated. The product composition at equilibrium calculated from the minimum Gibbs approach will be similar to Fig. 3.

It can be seen that, for this case, temperature and steam/ethanol ratio do not have an effect on carbon monoxide content. In addition, steam/ethanol ratio has less effect on hydrogen and methane contents compared to the condition with three reactions occurring (Fig. 1). When comparing with Fig.1, at the same temperature and steam/ethanol ratio, using catalyst with WGS activity provides more hydrogen and less methane. Temperatures above 800 K and high steam/ethanol ratio are still necessary for high  $H_2$  selectivity.

## 3.3 Low-temperature shift reactor

Since the ideal hydrogen stream to be used in fuel cell is to have very small CO content, for example, less than 1% for solid oxide fuel cell and less than 100 ppm for PEM fuel cell, further treatment of reformate is necessary. Such treatments include Low-temperature shift (LTS) reactor to convert CO to CO<sub>2</sub> at temperature around 200°C. In this part of study, the equilibrium composition of reformate obtained in section 3.1 was further analyzed for its equilibrium composition in the LTS. An important assumption is that the LTS catalyst is not active for other reactions. The plot of the composition in product stream after being treated in LTS at 200°C is shown in Fig. 4 with the x-axis as the temperature in reformer.

It is clearly seen in Fig. 4 that at low steam/ethanol ratio, the operating temperature in reformer cannot be higher than ~950 K to be used in solid oxide fuel cell. At high steam/ethanol ratio, the temperature can go up to 1073 K without CO problem. However, to be used in PEM fuel cell, reformer temperature has to be lower than 623 K at r=18, but low hydrogen yield would be obtained at this condition.

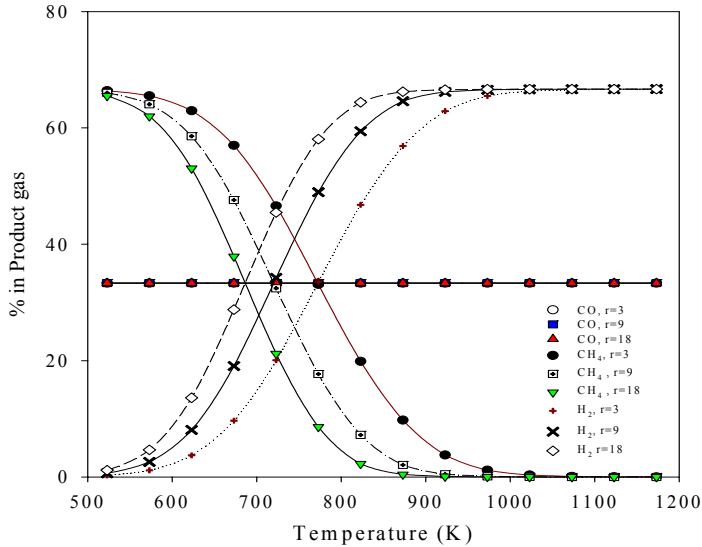


Figure 3: Equilibrium dry gas composition as functions of temperatures and steam/ethanol ratios if the catalyst is not active for water-gas shift reaction.

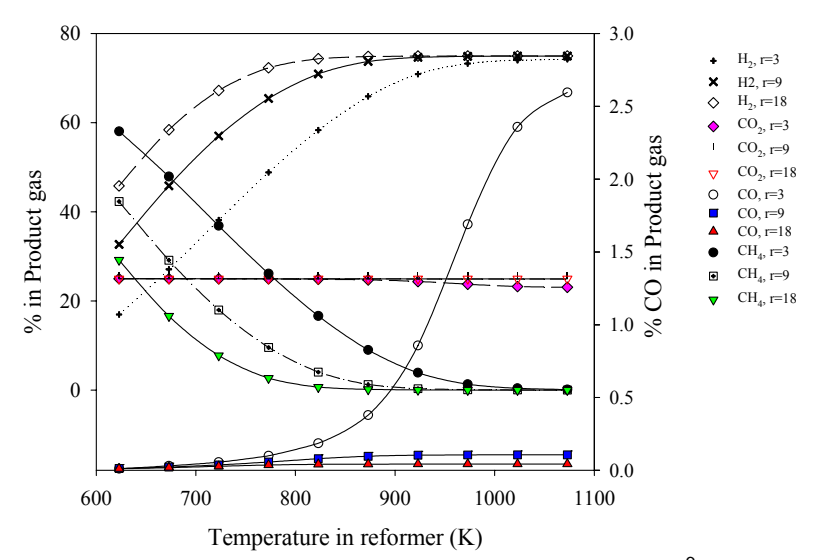


Figure 4: Equilibrium composition in Low-temperature shift reactor at 200°C using product gas from reformer at different conditions as feed.

## 4. CONCLUSIONS AND COMMENTS

Even though from the thermodynamic analysis, low-CO hydrogen stream can be obtained at high steam/ethanol ratios, when considering the reformer size, it might not be economically attractive. At high steam/ethanol ratios such as 18, the reformer size must be at least 4 times larger than normal reformer (r=3). In addition, higher heating and cooling rates are also required. Adding more reactors such as LTS and selective CO oxidation reactor might be more economically attractive. Therefore, excluding the condition providing low CO content and high hydrogen yield, future research should also consider the total cost and cost per unit of hydrogen produced.

### References

- 1. Mas, V., et al. (2006). International Journal of Hydrogen Energy 31(1), 21-28.
- 2. **Smith, J.M., van Ness, H.C., and Abbott, M.M.** (2005). *Introduction to Chemical Engineering Thermodynamics*. McGraw Hill, Singapore.
- 3. Comas, J., et al.(2004). Chem. Eng. Journal 98(1-2), 61-68.

## **Acknowledgements**

The authors would like to thank the Thailand Research Fund for all funding in this project.